CODEN:LUTEDX/(TEIE-5246)/1-50/(2007)

Industrial Electrical Engineering and Automation

Control of a Single-Phase Claw-Pole Machine

Alexandre Grandremy

Dept. of Industrial Electrical Engineering and Automation
Lund University

Control of a single phase claw-pole machine

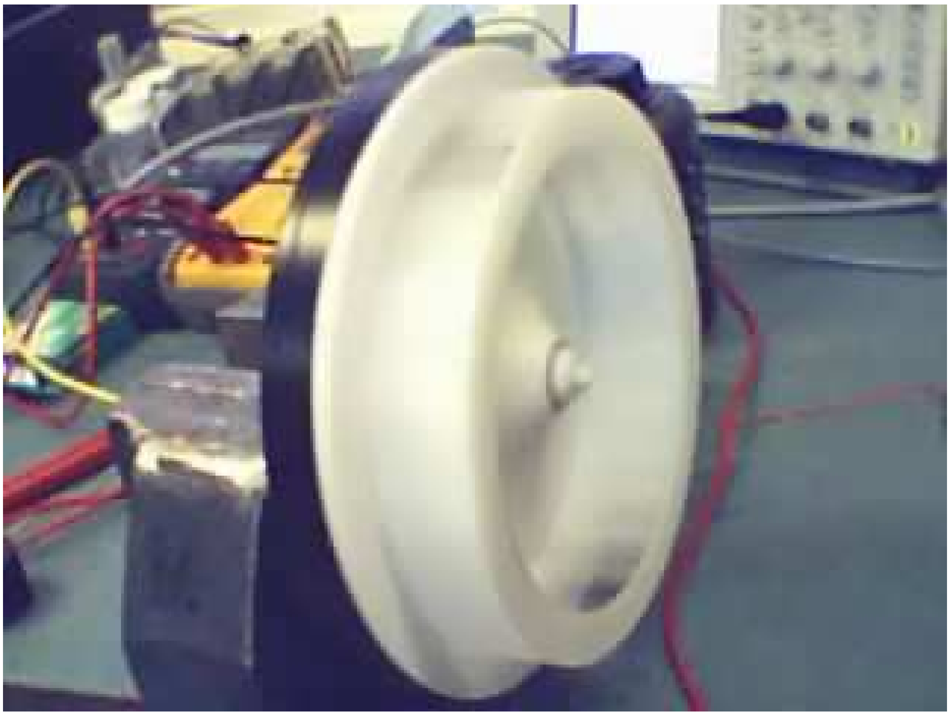

Master Thesis
by
Alexandre Grandremy

June 2007

Lund University INP Grenoble

Location: IEA *Industrial Electrical Engineering and Automation*
LTH Lund University
Supervisor: Avo Reinap, IEA LTH

Acknowledgement

First of all, thank you to Prof. Mats Alakula (IEA LTH Lund, Sweden) and Prof Jerome Mars (ENSIEG Grenoble, France) who trusted me and allowed me to carry out this Master thesis project within the IEA department in Lund, Sweden.

Everything that is good in this thesis is thanks to the inspiration and knowledge of my supervisor Dr Avo Reinap, who, in addition to be one of the best in his field, is also very enthusiastic and never saves his encouragements.

My special gratitude goes towards Getachew Darge, who made all the final experiments possible.

Special thanks to Johan Björnstedt for his help when using the dspace tool.

Thanks to the entire IEA department for welcoming me, and to my family and my friends all over the world for their support.

CONTENT

1 Introduction and Objectives of the work

The department of IEA Industrial and Electrical Engineering is carrying out several special projects on the design of unconventional hybrid machines under the great influence of Prof Mats Alakula and Dr Avo Reinap.

It is in this prospective that a deep research on single phase claw pole motor has been implemented leading to the construction of a prototype of stator whose main interest is to be low cost.

The master thesis somehow seeks to fulfil the next stage of this project, which is the control of this prototype of fan motor.

Unlike more classical motors, without control, this motor:

1) is not able to start by itself,

2) loses synchronism with any perturbations,

3) goes randomly towards both directions.

The cogging torque is partly responsible of these troubles.

A focus on this torque has to be first done before designing a whole control strategy to try and overcome these 3 problems and go through the seeking of high speed.

Will come after, the simulations of the actual machine showing some speed limitations to which some responses are designed.

Finally, the results of the total implementation are exposed and criticized.

2 The claw-pole machine

Even though the principle of electrical machines has been used for more than a century, their design is still subject to improvements nowadays.
These improvements are based on the use of relevant materials for the machine stator and rotor, their shapes and the process of manufacturing.
The single-phase claw pole machines that are under concern in this paper are evidence of this on-going progress.

2.1 Defining the claw-pole machine

The most well known motors in Electrical Engineering are the DC machine that is single phase, the 3 phase PM synchronous machine and the 3 phase asynchronous machine.
It is almost always all about a rotating magnetic field whose flux is somehow expected to be enclosed by the rotor.
In the 3 phase machines, the rotating field is a result of the combination of the 3 different sinus currents in the 3 phases. In the DC machine, a mechanical switch also called brush allows the different coils all around the shaft to produce this rotating field.

The single-phase claw-pole machine is neither of those, and it is a bit complicated to define.

The sure part is there are only 2 connections, that is, this is a single phase machine.
We can call it brushless because it only contains one coil which is buried in the fixed stator, and thus there are not any mechanical switches.
This coil is wrapped by the stator poles, which can be seen as 2 claws put face to face.
It belongs to the hybrid motors kind, the rotor uses permanent magnets.
It is not a DC machine because the fixed brushless stator coil is of course not able to create a space-varying magnetic fielding into the machine with a DC voltage.

So, how can it work if there is only one phase, the machine is brushless?

From a simplified magnet point of view, it is quite similar to a stepper motor, according to the sign of the current, the stator slot will be attracted to a north or south magnet, will provoke the first move and so on.

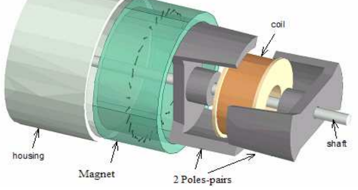

Figure 1 : Illustrating picture of a claw-pole machine

Basically, the principle is to provide pulses or alternative current to the coil so that it can make a space-varying field, and the rotor whose magnetization is also alternative almost like a sinus, can grab the synchronism.
This cannot be done without a perfect handling of the cogging torque and thanks to a well-designed control, as we will see in the following.

2.2 The iron powder stator core and its manufacturing process

The stator cores of electrical machines are basically supposed to be made of any material with a high permeability so that the flux could follow its paths with the smallest amount of loss, which is to say a small mmf drop and remagnetization loss.
A common material is laminated alloys of steel as it combines both the advantages of the interesting permeability and low eddy-current losses thanks to the lamination.
Nevertheless, it requires a quite demanding manufacturing process.
The Rotocast® method was created to remove this last inconvenient and it indeed does it pretty well.

The idea is to make a compacted iron powder core using the centrifugal forces. The iron powder is prepared and mixed with plastic adhesive, and the resulting mixture -*Figure 3*- is poured in the centrifugal machine -*Figure 2*- where the solid plastic cast equipped with the single insulated wounded coil of the future stator together has been installed.

When rotating, the machine, with the help of centrifugal forces, gets the plastic part of the poured mix separate from the mix drawing the outermost ring, while the iron draws the innermost ring filling up the cavities of the cast. Once the uninteresting plastic part removed, the result is a compact iron powder core whose shape is like expected.

Figure 2 : The Rotocast® machine

Figure 3 : Mixture under preparation

The first 2 visible advantages of this process is its lower level of complexity and its lower cost.

Indeed, in comparison, the usual principle using laminated sheets is a long and demanding process and appears thus much more costly.
Also, a larger scale prospective can be possible.

One other main advantage is that the design of the plastic cast, which forms the stator core, has basically no limit. Thereby, this machine can build round stator cores of any shapes, allowing the magnetic flux to follow any 3-D paths, contrary to laminated steel sheets still restrained to 2-D paths [1].

Thereby, it is possible to design machines of the radial, axial, circumferential, or transversal kind, this qualification referring to the direction of the flux in the stator core. Our claw-pole machine is of the last kind.
Two claw-pole machines are represented below -*Figure 4*-.

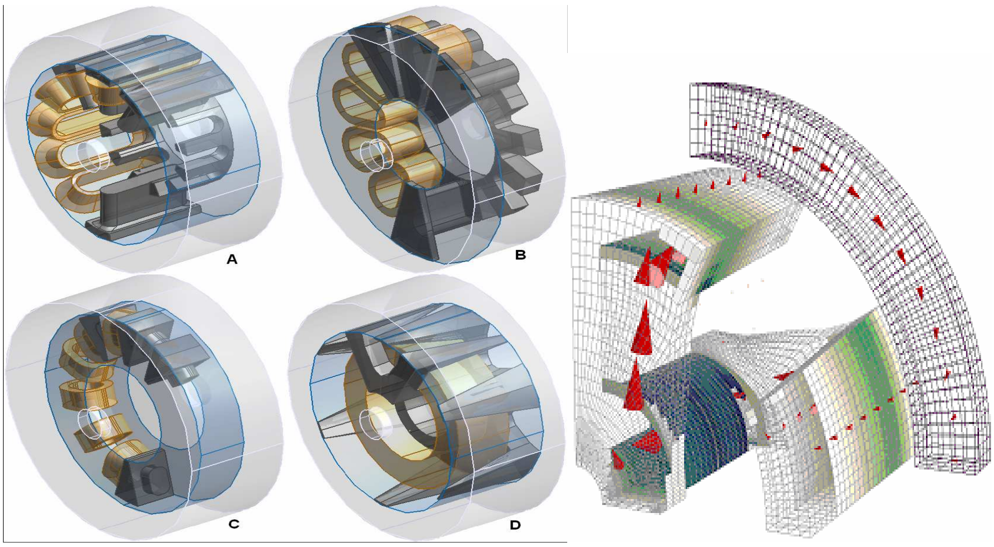

Figure 4 :
Rightmost : A: Axial B: Radial C: Circumferential D: Transversal Claw pole Machine
Leftmost: Representation of the flux way flowing through the different parts of the claws via the rotor for a 4 poles claw-pole machine

These advantages widely compensate the inherent lower permeability of the iron powder cores µr#13 for our Rotocast® cores, and make them interesting subject of researches.

2.3 The rotor and its magnet ring

The set {rotor/magnets} used is not common either.
There are basically two types of permanent magnet (PM) machines, based on the location of the stator and the permanent magnets. One is called *outside rotating* and the other, *inside rotating.* As the name implies, the outside rotating machine employs magnet poles rotating outside the armature winding. The inside rotating motor is similar to conventional PM motors, whose rotor rotates inside the armature winding.[2]
Our claw-pole machines are of the first kind less conventional

The other singularity of this set does not come from the outermost part which is a typical electromagnetic conductor. But it comes from the magnet part. The latter is indeed not consisted with a certain number of magnets incrusted or buried in a material. But it is an elastic band or magnet ring made of ferrite NdFeB (Br=0.24 T), that seems like natural rubber, and we can fashion at our will the magnet ring, by cutting and assembling different pieces of it.

2.4 The actual machine to control

A deep research on the design of these claw-pole machines has been implemented by Avo Reinap at IEA, whose one of the purposes was to determine, for such a material, which dimensions and geometry could be the best compromise between all the relevant factors (thermal, mechanic and magnetic aspects), within the given dimensions.

This is according to this prototyping study that some stators had been built, and the 20 pole-pairs stator of the machine I have to control is part of them -*Figure 5*-.

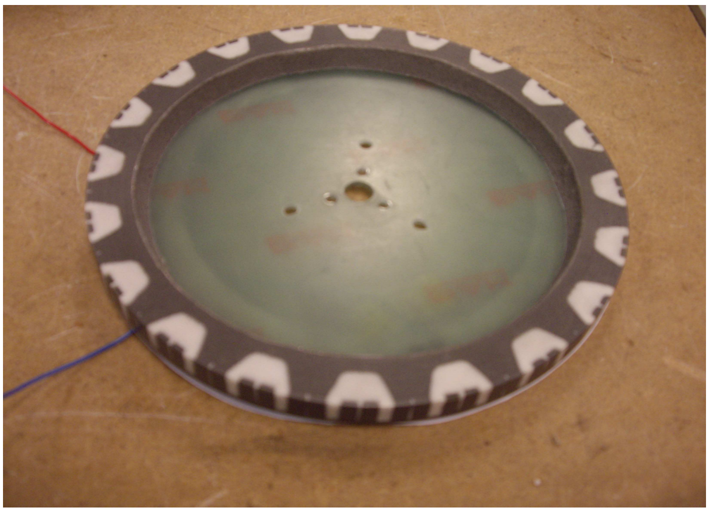

Figure 5 : Stator of the actual machine

However, the design of the magnet ring is free of change in the following of the project -*Figure 6*- since the magnetization features of the magnets are not clearly known- their shape is selfdetermined during the design process- and because it considerably affects the cogging torque and the control of the machine.

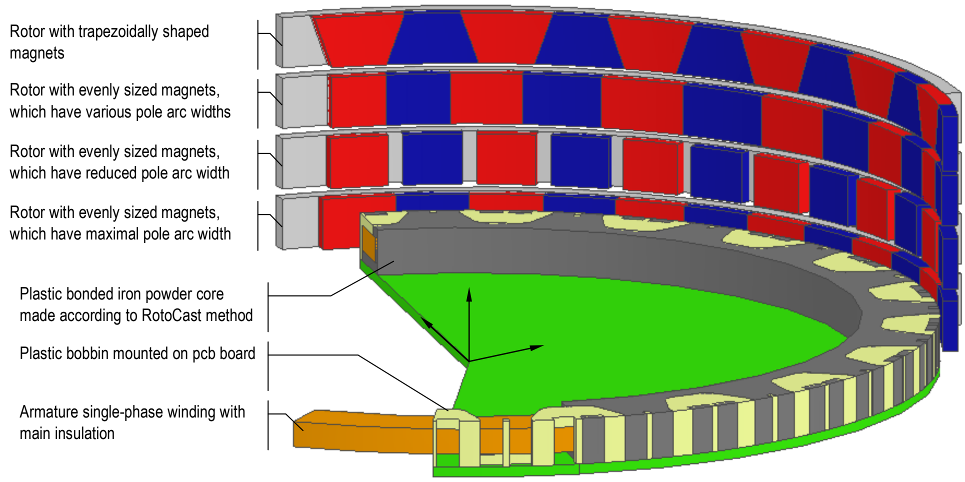

Figure 6 : Examples of magnet rings with the actual stator

3 The Cogging Torque

3.1 An additive static torque to be handled towards 3 purposes

When handling the rotor of such a brushless PM machine at unloaded conditions, one can feel that there is an opposition to move it forward or backward, there are some positions where it is easy to move to, although there are some that are very difficult to reach.

This is the result of a static torque, that we could call “no current torque”, which is inherent to every PM machine. In other words, whatever the electrical and mechanical conditions, this torque component remains the same and is additional to the drive torque which is proportional to the current.

This non-current torque is allegedly called “detent torque” or “cogging torque” depending whether it has a positive effect – detent – or a negative effect – cogging –.
The main example of the positive one is the stepper motor application, in which this static torque kind of holds or “detents” the arm at a fixed position.
Yet, in most of the conventional applications, it has an undesired impact because it causes speed ripples or cogging motions, which can also trigger an important noise.[3]

This inherent characteristic of PM machines originates from the interaction between magnets, as well as between the different magnetic poles.
One first way to face it is to see it from an energetic point of view.
Every physical system has a natural propensity to minimize its energy. That is why the pendulums have their stable position down at the vertical where there is no potential energy. The

upward vertical position is another equilibrium point but unstable because too close of high-energy areas. -*Figure 7*-
This is basically the same situation with our magnets and the cogging torque. The magnetic flux always flows around closed circuits. The shorter the circuit is, the smaller the energy gets. Thus, stable positions are these points where, in a way or another, flux circuits are the shortest. Like positions A and B for instance -*Figure 8*-.
Other equilibrium points similarly show up but they are too close of higher energy areas.
Away from these stable positions, the magnets are like attracted to get back to these positions.

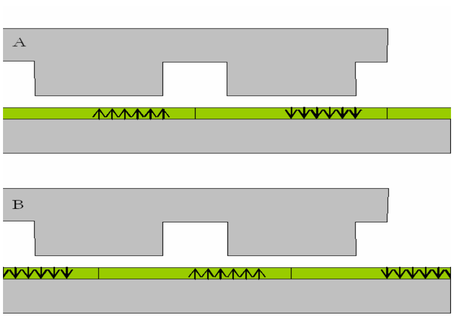

Figure 8 : Example of stable resting positions

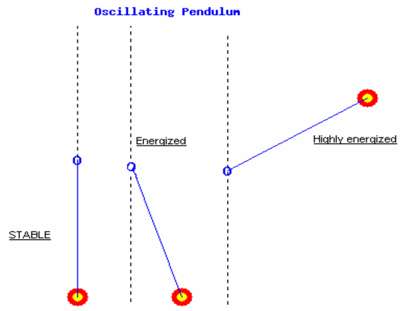

Figure 7 : Example of the pendulum

This torque is a function of the mechanical angle, and should be periodic, and whose scheme is totally included in 2 π electrical angle.
The period, the waveform and the level of torque depend almost on every single aspect of the design. As a matter of fact, the number of poles and magnets affects the periodicity and the waveform; the magnetic nature of the material, its permeability scales its level.
Yet, the cogging is thus very sensitive to every change in both the material properties and geometry of the stator, and the repartition of the magnets, as well as their interaction.

It has a tremendous importance simply because it is supplementary to the drive torque. As a matter of fact the drive torque is twice zero over the period. Therefore, detent torque can modify totally the waveform of the total motor torque, which allows the expected motions. It can create unexpected peaks, reduce consequently the torque level at some positions, and shift the zero-torque positions, which matters when it deals with starting-up the machine.
Also, the cogging torque is assumed to be permanent whatever the electric conditions, and thus will finally not provide any energy to the system, but can reduce it if not well handled.
Furthermore, the unwanted cogging motions I referred to above gets as much important as the cogging peaks get high.

So, all the design and the simulations have been oriented towards 3 main targets:

- feasible and best starting-up conditions
- minimum cogging torque
- maximum drive torque and ratio drive/cogging

3.2 Cogging and Self-starting

Given that the cogging torque is present before running, it actually imposes the position where the machine will stop, the so-called resting positions.

These positions are defined by *Tc=0 N.m* and by its derivative negative $\frac{dTc}{d\theta} < 0$.

-*Figure 9*-.

The "zero positions" with $\frac{dTc}{d\theta} > 0$ are unstable.

Section 4.1 will go further and clarify on this last point.
Meanwhile, the electromagnetic torque Td draws its own periodic figure, generally close to a sinus, with its own zero positions with $\frac{dTd}{d\theta} < 0$.

If they correspond to the resting-positions, the total torque is null Tt=0 N.m and $\frac{dTt}{d\theta} < 0$ and the self-starting is thus impossible. See Case (a) -*Figure 9*-.
So, to ensure a possible self-starting, every resting position should correspond to a sufficient level of drive torque to overcome the magnetic and mechanic frictions. See Case (b) .
The best conditions happen of course when the absolute value of the drive torque is the highest at these points [4].

Besides, if we invert the problem, if there was no detent torque, the total torque when electrically loaded would just be the drive torque with zero torque positions with negative derivative every half electrical period or 180° on the figure case (a) and (b)-
At these positions, no self-starting would be possible.
Therefore we can figure that the cogging is at a certain level needed for what we could call "starting positioning".

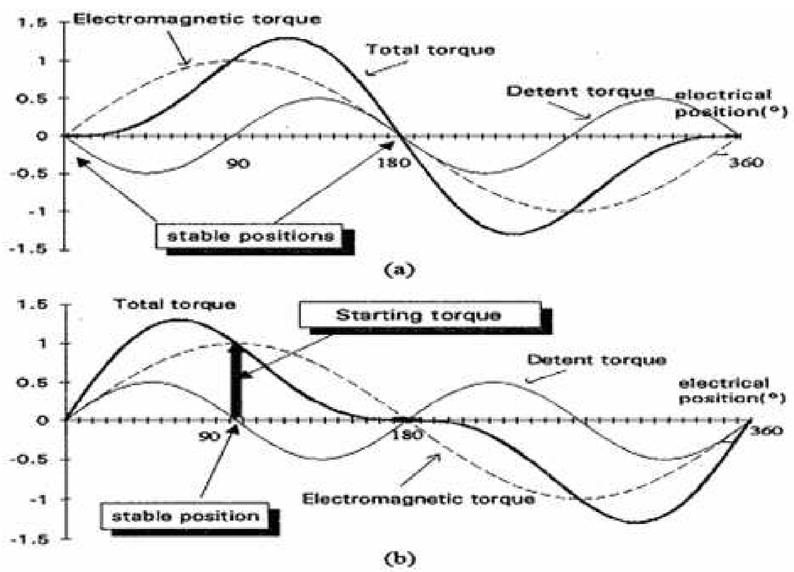

Figure 9 : Simplified example of electromagnetic and detent or cogging torque variations as a function of the rotor position
- (a) impossible starting - (b) possible starting

3.3 The pursuit of the 3 purposes

The optimizations – e.g. the minimization of the cogging and maximization of the ratio drive/cogging – are a complicated processes because they are multi-variables.
Based on FE calculations and simulations, estimating the magnetization patterns of the magnet ring, some choices in the design of the stator have been made:
-The relative pole width, that is the ratio "pole width/maximum pole width" is fixed with the stator construction.
-No poles shifting was implemented here, the poles are evenly displaced around the stator.
-The claw-pole division into 2 halves is done to reduce the cogging torque peak, but also to increase its periodicity.

The cogging also depends considerably on the magnet ring, more exactly on the repartition of the magnets, and their matches with the stator plots.
Moreover, since the magnetization pattern and material parameters of the magnets are just approximately known, the real cogging torque can be quite different from the one estimated.

This is why it is of the biggest importance to measure the cogging torque, to check if it is close to what was expected, figure out what happens in reality and learn from it, to check the feasibility of the starting up and the level of the torque peak, and eventually try to improve the design of the magnet ring towards the final targets.

It is in this R&D prospective that I implemented several measurements, which are being exposed below.

3.4 Measurement

3.4.1 Measurement methods

The measurement part is crucial and so the methods used for that must be well thought and tried.
That is why some methods or improvements are first developed on a small claw-pole machine whose simulations and measurements had already been done.

Several factors matter more when it comes to measurement:
the feasibility, the accuracy, the relative simplicity, the cheap cost etc…

Thereby, developing such a method opens a quite big place to imagination.
It is all about having ideas, evaluating the degree of complexity, minimizing an eventual cost and the time spending on it, and eventually use if possible only the available material in the labs.

As the small claw pole and our concerned machine is 20 pair-poles and is symmetric, the periodicity of the cogging torque is likely to be of 360/20=18degrees.
Nevertheless, the symmetry is not perfect, and it is anyway better to considerate several periods for our investigation.

Anyway, in order to get reasonable and exploitable measurements, either angle and torque measurement system should give the best accuracy possible.

The “ideal” solution coming first to my mind is to plug the machine into a calibrated DC machine through a common shaft. The machine would be position controlled, and run with d-Space, we would have access to the torque of our examined machine by the torque of the DC machine directly proportional to the current flowing into it.
Even though it would certainly give a good accuracy, it disqualified for a lot of reasons whose first ones are the high complexity and the gathering of many devices.

In regard of simplicity, the following weighting-scale method [1] sounds way better.
The solution is to find out the point of mechanic equilibrium thanks to a load mass *m* or setting up the position θ *-Figure 10-*.
The mechanic equilibrium is actually the balance between the cogging torque applied to the rotation axis and the load applied to the arm of the beam.
The common cases of unequal weights are arranged by introducing the angle δ between the horizontal and the position of the arm whose length is l.
Therefore, the cogging torque is calculated as follows:

$$(1)\ \mathrm{T}(\theta) = 9.81 \cdot \mathrm{l} \cdot \mathrm{m} \cdot \cos(\delta)$$

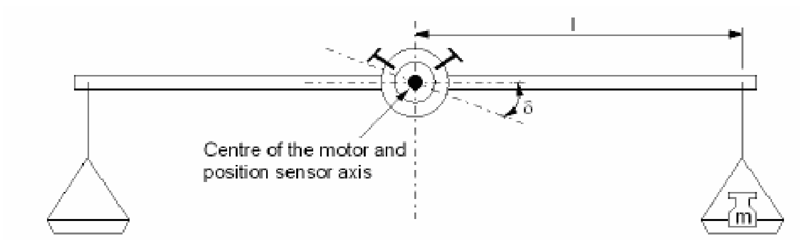

Figure 10 : Weighting-scale measurement

Two types of errors are introduced in the measurement. One of them is the measurement accuracy of the position and the other is the estimation error of the load torque.

Starting from the 1st method described, instead of estimating the torque, it can be measured with a dynamometer. Indeed, linked to the rotating part with a nail, it gives the tangential force triggered by the cogging torque, while we can measure the angle. This way simplifies the calculation of the torque- the value read on the dynamometer will thus be directly proportional to the torque with factor the radius r of the circle of which the force is applied to - and permit not to build a special beam and swing for that.

Anyways, the angle measurement is still the main problem, as it has to be done on a small range of angle of 18 degrees.
A very simple tool to measure it is built with the help of a big protractor. This quite large half circle is fixed and centered into the middle of the shaft. Its size gives a pretty good resolution.
The arrow is done with a plastic beam, perfectly centered on the middle of the motor, and free to rotate. *-Figure 11-*.

To improve the angle measurement device a better scale printed with Matlab is used. The resolution is thus 0.5degrees, which is acceptable given the size of the circle.

The reading is done with a nail as an arrow on the beam, which is pointing at the right angle, as the dynamometer reveals a certain value of force.

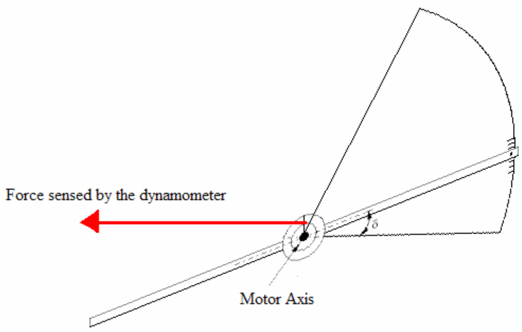

Figure 11 : Dynamometer Measurement

Another idea to improve further the angle accuracy was to dig a tiny hole in the beam, and to light through it with a lamp. Thus, a small and precise lighted point shows up on the angle scale, which makes the reading as convenient as accurate.
The only point is to keep the light horizontal and faced to the beam so that the ray is horizontal.

To be able to do the measurements by myself, the dynamometer is fixed to an heavy box so that a value of force can be chosen, sliding the box on the measurement table, and the measurement system remains stable and the angle can be read carefully.

This method, despite its homemade look and discussable accuracy, have shown very good concordance with the previous measurements and simulations on the small claw pole machine, so this is the one that will be used for our machine.

3.4.2 Measurements and observations

The purpose being to determine precisely the torques and get the understanding of the behavior of the machine, the measurements and the observations must be very complete.
For each magnet ring, 3 series of measures per given range of angle, and for every electrical condition:

- machine unloaded to get the cogging torque itself,
- machine loaded with different current, negative and positive, to get the total torque-drive+cogging torque- waveform. The supplied current is around 1 or-1A which is the nominal current.
- Some more observations are done feeding a quick impulse of 1A or –1A, also, the machine is run with 50Hz sinus current, after having grabbed the synchronism.

The areas with a positive derivative are unstable and it is thus impossible to measure these parts of the torques characteristics.

Nevertheless, by handling the machine, we can determine these unstable points where the machine wants to reach the backward resting position if slightly backward, and forward otherwise. So these parts of the following curves are the result of estimation and use of cubic interpolation.

3.4.2.1 Magnet Ring 1

The magnet ring number 1 is designed with progressive width pieces of ferrite magnet stack displaced as follows. See also -*Figure 6*-:

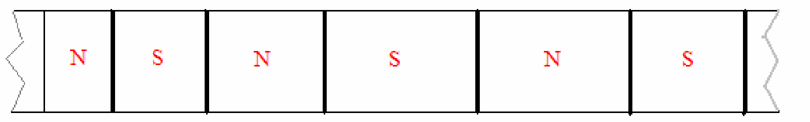

Figure 12 : Magnet Ring 1: Evenly sized magnets, which have various pole arc widths

This combination is supposed to reduce the cogging torque.

The result of the measurement for the total torque and the cogging torque is plotted below with cubic interpolation, as well as the result of the subtraction of the cogging to the total torque that is supposed to represent the drive torque.

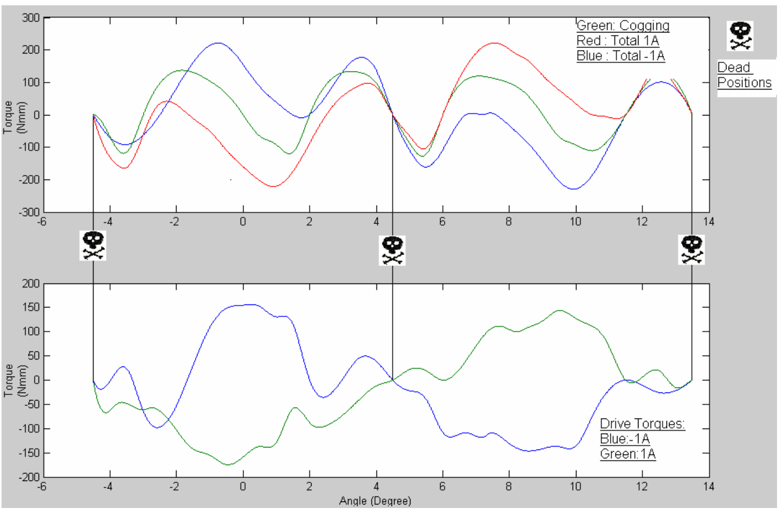

Figure 13 : Top: Cogging and Total Torque of Magnet Ring 1
Bottom: Drive torque

The slightly curious parts in the shape of the drive torque – for example around 2° – are certainly the result of the presence of magnetic and mechanic friction, the lack of accuracy in the measurement, and mainly due to the estimation of the unstable areas and the interpolation treatment.

From the measurements, we figure several observations:

- The cogging torque in itself reaches its stable positions every 4.5 degrees
- On some stable positions, the machine does not move when applying instantaneously 1A. The occurrence takes place every 9 degrees. In the measured range, they are –4.5, 4.5 and 13.5. Actually, they are passive stable positions or “dead positions”. From these positions, the machine can’t start up without exterior help. From the active stable positions the motion can be activated and from the passive stable positions it cannot be.

The magnet ring number 1 immediately disqualifies because of the presence of passive stable positions and so an impossible self-starting.

3.4.2.2 Magnet Ring 2

The magnet ring 2 is designed to be without passive stable positions. The idea is to reduce the cogging torque frequency and it is now made with evenly sized trapezoidal pieces of magnets, displaced as on -*Figure 6 and 12*- so that there are no passive stable positions.

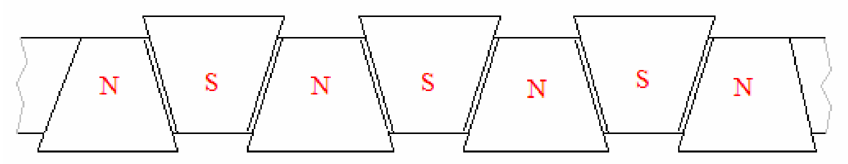

Figure 14 : Magnet Ring 2 : Trapezoidal shaped magnets

The result of the measurement for the total torque and the cogging torque is plotted below on -*Figure 13*-. The result of the interpolated subtraction of the cogging to the total torque supposing to represent the drive torque is plotted

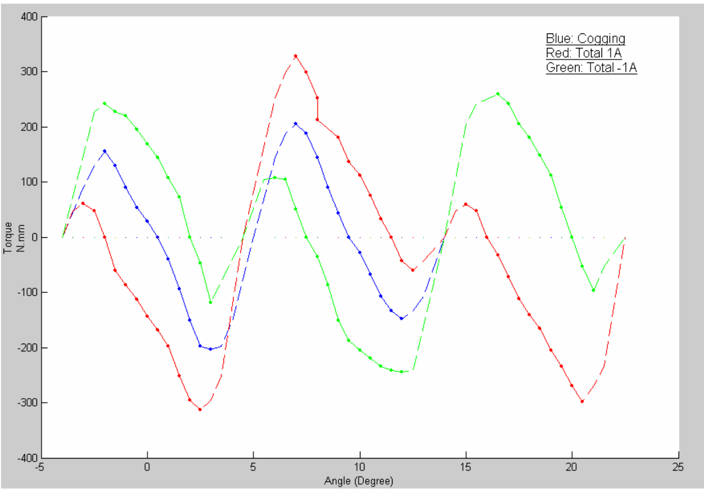

Figure 15 : Cogging and Total Torque Magnet Ring 2

ıt:

- The cogging torque resting positions show up every θ#9 degrees, the frequency is lower.
- Like expected, when applying instantaneously some currents from any stable positions the machine no longer keeps immobile. In other words, the machine doesn't have passive stable positions anymore. This is what we wanted.
- The cogging torque peak level is much higher than for the magnet ring 1 like expected. Numerically it is around 1.5 times higher

To put it in a nutshell, even though the cogging is higher, the magnet ring 2 qualifies for the control because of its good self-starting conditions.

4 The Control of the machine

From a good understanding of the cogging torque dynamic 4.1 on a similar but smaller claw-pole machine, is designed a special control strategy 4.2 based on a position area detection 4.3.
4.4 introduces different complete control systems based on the former control strategy that are simulated or implemented in practice in Chapter V and VI.

4.1 Understanding of the dynamic mechanic of the system

To be able to design a control of the machine, it is important to understand the dynamic of that kind of alternative torque like the cogging torque.

Therefore, as a first step, only the dynamic of the unloaded motor is studied, that is, only the influence and the dynamic of the cogging torque when it is left from several non-resting positions.
To do so, a simple model representing the mechanic equation (2) is built on simulink. It takes into account the damping D. The friction torque can be either neglected or considered as together with the Damping effect.

(2) $J\frac{\partial\Omega}{\partial t} + D * \Omega = Tcog(\theta) - Tfriction(\Omega)$

For the cogging torque, 2 different models are used.
As the cogging torque is usually not that different from a sinus, periodicity equal to the angle between two magnets, that is 2*pi/N with N the number of magnets, it is first approximated and modeled that way, using a maximum torque roughly in the same range to the one measured for the small claw pole-machine, that is,

(3) $Tc = Tcm \cdot \sin(N \cdot \theta)$ with Tcm =0.01Nm

The second model uses the measured values (called ‘vm’ below) interpolated over a period.
Both models ‘sin’ and ‘vm’ are run with different initial positions to see their influence and to understand the dynamic going on.
Below come altogether the cogging torque versus the angle and 3 different time-evolutions of the angle, when left from 3 different positions chosen in different parts of the torque characteristic {0, 0.5 , 3}

-*Figure 16*- and -*Figure 17*-.

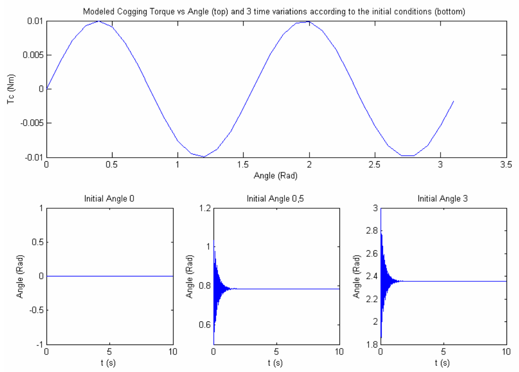

Figure 16 : Sinus Cogging and Evolution from several positions

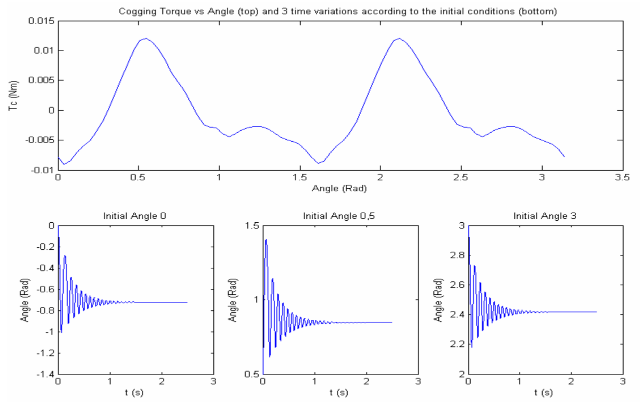

Figure 17 : More Practical Cogging and Evolution from several positions

In most of the cases, like it appeared during the measurements, it acts like a damped oscillator.

When starting from the unstable position of zero torque, which is zero in the sinus case, there is no move. This result is not wrong but it is actually a pure theoretical result since, it is usually very difficult to put exactly this initial condition handy. Indeed, in reality, when placing it even extremely closes to zero is enough to make it rotate and to get the propensity to go to the next stable position of zero torque.
Similarly, a pendulum placed on the vertical upward position is moving in practice.

Zero is no longer a no torque position in the second model and then it starts oscillating to reach the closest stable position.

Having a look at the cogging characteristic, and pointing at the initial point we can figure well what is happening in every case:

For example, let us start from the second and third sinus case. The position 0.5 provides a quite big positive torque to the system, and so the motor is rotating forward, the angle is increasing over $\pi/4$-the stable zero torque position-, where the torque gets negative. The inertia allows the rotor to continue in the negative side, but the negative torque and the damping stops the increase of the angle. At this point, the angle is maximum, the speed null and the system is like left from this last position. Thus, the same phenomenon is unfolding again but in the other sense. Indeed, as the torque is negative, the angle is going to decrease and so on. The angle finally describes a damped oscillation. This is basically the same situation when the initial angle is 3 except that the torque is negative at the beginning, and that it oscillates around the other stable position $3\pi/4$.

One can notice the difference of responses between the 2 models. In the less theoretical second case, the responses are no longer damped sinus, but the carrier waves maximum describe 2 exponentials not as regular as in the sinus case and the exponential factors are different according to the positive or negative sides.
Furthermore, the irregularities of this measured torque somehow induce some kind of harmonics (exactly like in electrical networks when this kind of non-perfect sinus is supplied to some passive loads) in the position and the speed.

4.2 Synchronization Control strategy

We can now apply this understanding taking also the electromagnetic torque into consideration (4).

$$(4)\quad J\frac{\partial\Omega}{\partial t}+D*\Omega=\{Telm(J,\theta)+Tcog(\theta)\}-Tfriction(\Omega)$$

The total torques taken from 'vm' when the current is maximum 1A, zero and minimum –1A (the meaning of maximum is related to the measured values but 1 A is also the nominal rated value) are plotted below -*Figure 19*-..
To have a look at the drive torque waveforms, the total torque minus the cogging torque is also plotted below. -*Figure 18*-.

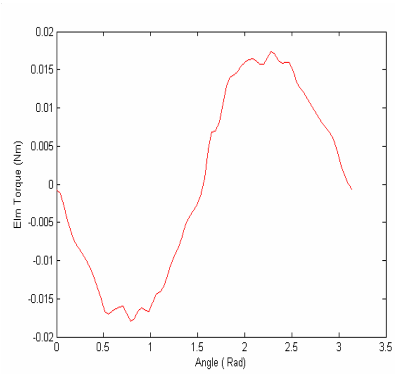

Figure 18 : Drive Torque in the model

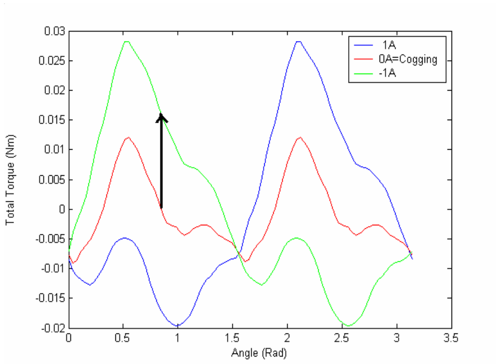

Figure 19 : Cogging and Total Torques in the model

From the electromagnetic torque figure, we notice it is nothing but a common electromagnetic torque waveform, that is, almost sinusoidal.

From the rightmost figure, we observe that:

- we obviously find back the cogging torque when I=0A
- the total torque still contains the cogging torque, but shifts the position of zero torque and the stable positions, like we saw in the chapter III).
- the waveforms from –1A and 1A are angle shifted of half a period, more generally, the inversion of polarities shift the Total Torque from half its period.

From a stable position of this motor at rest (0A curve), which is zero torque and whose derivative is negative, if we apply -1A to the winding, the torque is no longer null and gets a positive value-follow the black arrow on -*Figure 19*-. Then, without any further changes, this is basically the same situation than with the cogging torque only, that is, the motor gets the propensity to go forward to join the next stable position of the total torque.

Therefore the motor could not rotate with DC current. But, if the polarities are changed before it goes to the stable position, at some well-chosen moments, then it switches and jumps to the other curve, and the torque can get positive again. The amount of energy gained by the system and the inertia allows the system to go through a little period of small negative torque.

More simulations in which selected low frequency square current is supplied to the system lead to the result that it can effectively make rotate the machine
50 runs are implemented with the period T varying from 0.01 to 0.5s, that is from 100Hz to 2Hz, calculating the average speed and the ripple.
The only remaining good frequencies, frequencies which actually both triggers the rotation and do not imply an unacceptable speed ripple are within this area [20 Hz / 40 Hz]. Below is the result of the average speed according to the frequency of the square signal.

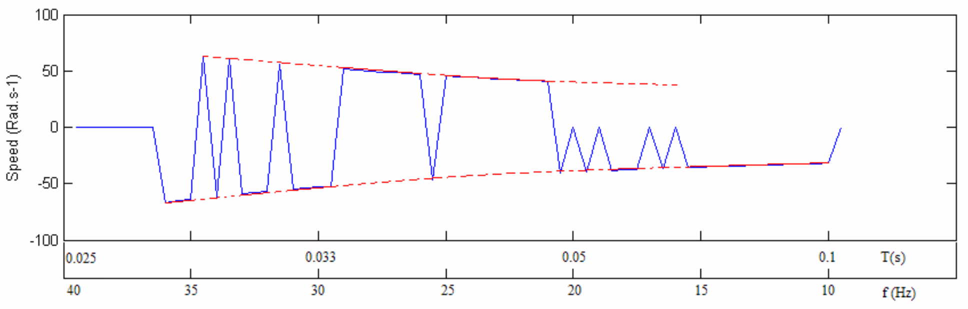

Figure 20 : Average Speed versus Electrical Period

We can figure that in these cases of rotations, the machine is almost perfectly synchronized.
Indeed, we can figure an inversely proportional relation between the speed and the electrical period, and we find back that the machine simulated gets 2 pole-pairs by verifying Speed#2*Frequency.

However, in addition to the very small area of starting frequency plus the fact it loses very easily the synchronism, the sense of rotation is like random.
Therefore, these theoretical starts are only a matter of chance.

To avoid all this uncertainty, the matter is to process these alternative pulses exactly when they are needed according to the torque characteristics.
We always expect a machine to produce the maximum torque, thus the polarities should be changed at such moments so that the machine gets the smallest amount of negative torque and the biggest amount of high positive torque, in case of a forward rotation.

For instance the best choices to invert the polarities in the case of the small machine -*Figure 21*-.would clearly be around 0 rad 1.6 rad and Π rad.
For a forward rotation -1A should be supplied between 0 and 1.6 rad and 1A until Π rad and so on…
The exact opposite situation for a backward rotation.

Below is represented the same figure with this configuration indicating the torque way the machine is supposed to follow.

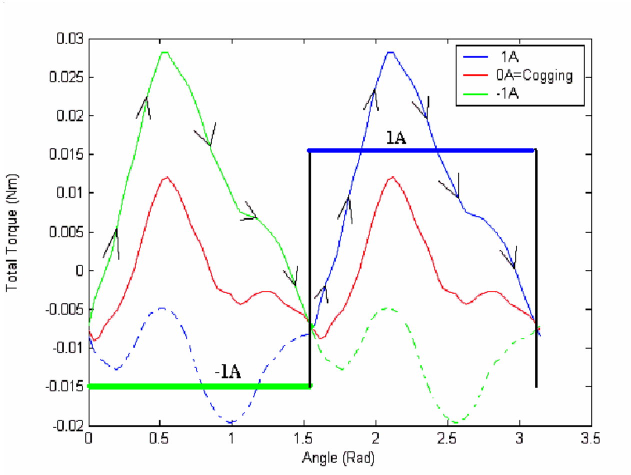

Figure 21 : Cogging & Total Torque, the ideal current pulses and the way the machine would run along.

The very good points of this method, is that it theoretically totally answers to every purpose.

Indeed, this way,
1) The machine could get started,
2) The sense of rotation could be chosen and on demand.
3) Last but not least, it would not lose synchronism. Indeed, we see that this dependence on the position area makes the control robust, that is, a change of load torque or some more damping effect won't affect the good run of the machine, as the polarities changes will still occur at the good moment.

All these points are checked and illustrated through simulations on a simplified model , representing the equation (5):

$$(5)\ \ J\frac{\partial \Omega}{\partial t} + D * \Omega = \{Telm(J,\theta) + Tcog(\theta)\} - Tfriction(\Omega) - Tload$$

-*Figure 22*-. represents the starting, and -*Figure 23*- represents the synchronization keeping.

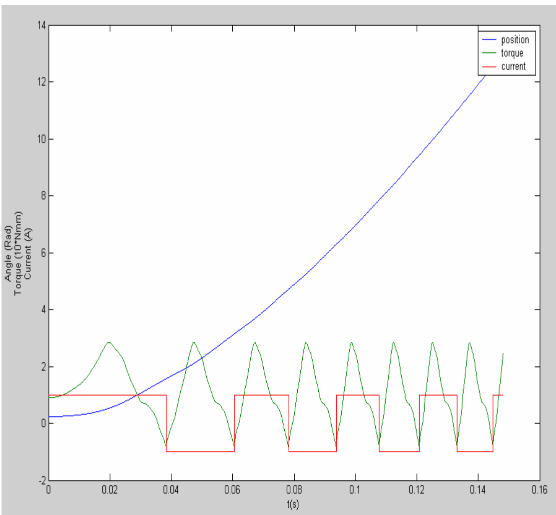

Figure 11 : Validation of the starting with the Synchronization strategy

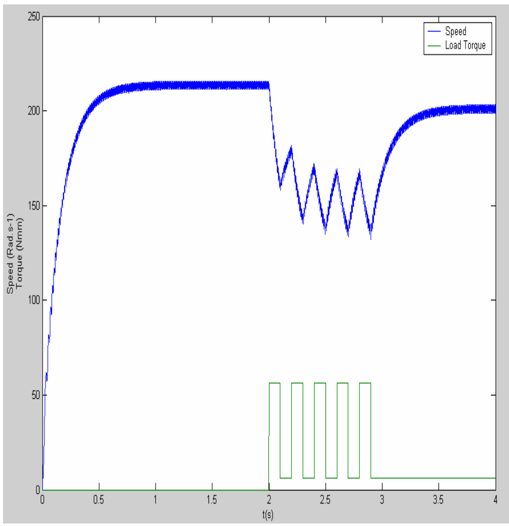

Figure 12 : Validation of the Synchronization keeping

This is very simplified because none of the electromagnetic and electric conditions are taken into account, and the system gives the expected current pulses without any delay.

However, this simplified model shows good result towards the 3 purposes and ensures the first step of validity of this strategy.

So, generally speaking, the synchronization control strategy of such motors would consist in giving alternative current pulses in the appropriate position area.
Below is how it actually looks like with the real machine and with the measured torques.

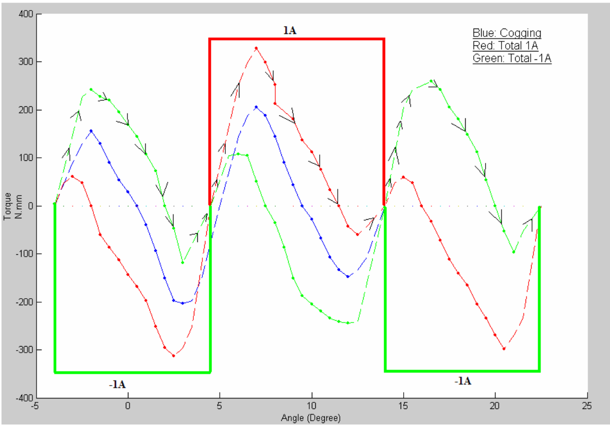

Figure 24 : Synchronization strategy and actual machine

Therefore this control needs a sensor that must be able to determine in which position area the motor is and therefore communicate it to the rest of the system so that the right electrical conditions can be set.
Like other motor control, an appropriate power electronics circuit like a 4 quadrant circuit can be used to switch polarities whenever it is needed.
Below represents the first perspective of this synchronization control.
The position area sensing is discussed in the next section.
The solutions for the Switch trigger signal building will be discussed further in 4.5.

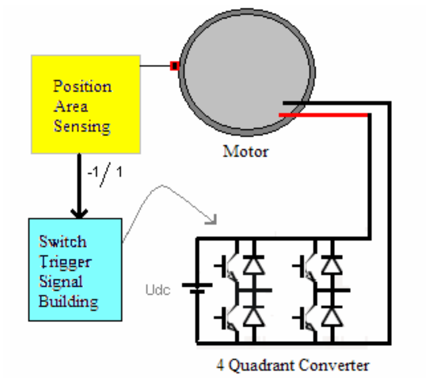

Figure 25 : Synchronization Control

4.3 Position Area Sensing

4.3.1 Choice of a method

Like when developing a measurement method, some main factors must be taken into account when choosing a position area sensing solution:

- It should be simple and should not require any additional construction of the machine.
- The cost should be small since it is supposed to be a low cost application.
- The time response should be as small as possible, so that it won't shift too much the ideal pulses positions.
- It must be precise so that the detection of the 9° wide area will be fine.

An unexpected shift or change of polarities at the wrong moment can get the torque negative for a while and could brake the machine or worse make it lose synchronism.

The usual position sensors that are shaft contacted disqualify since the machine does not have any shaft.

The optical technology disqualify because of its expensiveness.

Some control applications of 3-phase machine based their control on the use of several magnetic field sensors from 3 to many more place on some strategic position.

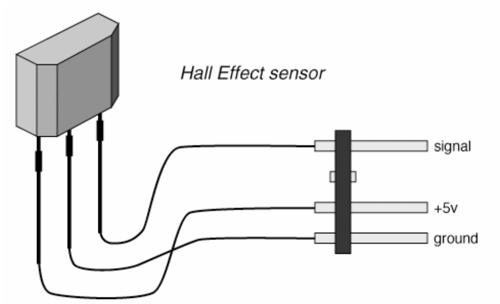

Figure 26 : Hall Sensor and its connections

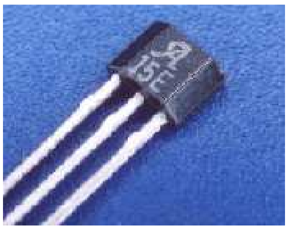

Figure 27 : Hall Sensor

Given the cheap price, the simplicity, and the suitable characteristics of the Hall sensor, a study is led to develop a method that could use the leakage magnetic field as position information.

The analysis of the Permanent magnetic field evolution both in the small machine modeled shows that the angle periodicity of the ideal polarities changes and the one of the supposed PM Field sensed are equivalent. -*Figure 28*-
Besides, in this case the ideal polarities changes seem to correspond to the absolute maximums of magnetic flux.

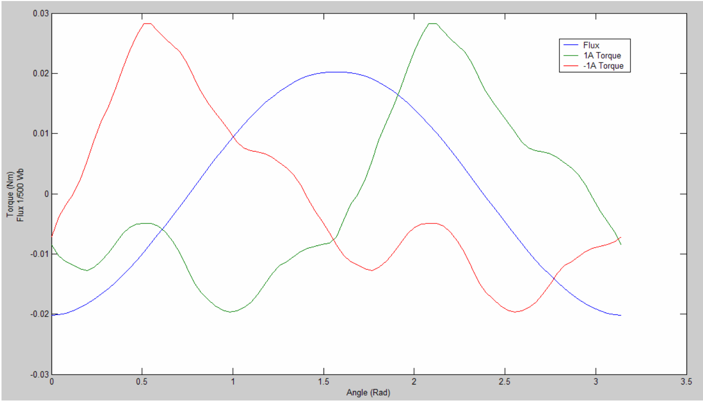

Figure 28: Match PM Flux and Total Torque

Then, it is not necessary to measure the angle. Indeed, given the periodicity match, the magnetic flux at one precise place over the stator or the air gap can give the essential information with or without signal treatment, to determine whether positive or negative current should flow into the motor coil.

From all these information, the first idea is thereby to use only one sensor well positioned, and to associate it to a derivative filter, and to an hysteresis amplifier centered on zero ordering positive current if dB/dt > 0 and vice and versa.

Yet, handling a derivative signal is never obvious and it gets even tougher regarding the stability when the signal comes noisy.

To avoid this derivation process, a second solution based on 2 sensors, displaced evenly distanced from the middle of the stator pole, is also considered:

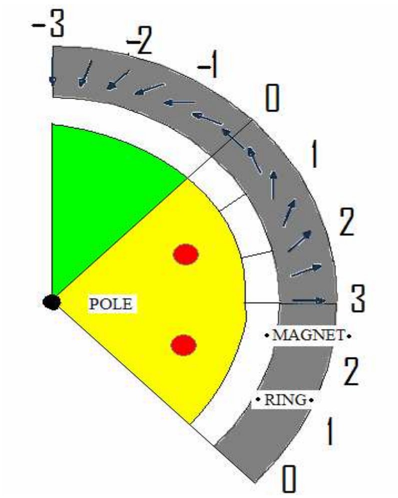

Figure 29 : Possible placement of 2 sensors (Red Spots) over a stator

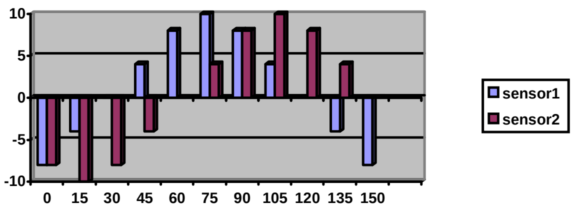

Figure 30 : simplified representation of these sensors information in this configuration

To make -*Figure 30*-, it is assumed there are 6 different levels of flux in the magnet ring -*Figure 29*-. It is also assumed that the sensor feels mainly the flux right in front of it – a coefficient 2 is weighed for this position – but also depends on the flux right besides – a coefficient 1 is affected to these ones –.

Thus, in the case of the first sensor -*Figure 29*-, the level of flux sensed is Fl=2*1+1*(0+2)=4 (no unit).

The idea is that both sensors will see the same information with a certain shift of time.
Then, the information 1 and 2 match at the particular points where a unique sensor would have its maximum, that are, the supposed ideal positions of polarities changes.
Therefore, subtracting them give a resulting signal whose zeros would correspond to the polarities changes.

However, this method put forward at least 2 drawbacks:
The need of precision in the placement that cannot really be easily handled, as well as its inconvenience when the pole width is too small.

Whatever the solution chosen, it appears quite clear that those sensitive hall-effect sensors should be carefully positioned.
Also, there is always a shift between the expected theoretical results and the reality of practice when it deals with magnetic field with sensing devices.
Thus, in order to determine the most suitable sensing position, a positioning study is implemented via dspace.

4.3.2 Positioning Study

First of all, even though the leakage field must be stronger over the air gap, this idea is left behind, since the device can be subject and exposed to damage.

On the plastic part, we can basically distinguish 3 distinct areas over which we can place the device-see –*Figure 31*- above-

1: Over a pole not far from the air gap
2: Over the iron belt common to every pole,
   that is, over the part where the coil is buried
3: Over the teeth from the opposite poles

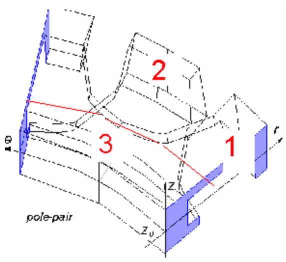

Figure 31 : Sensor Locations

Several conditions are applied:

- A : non loaded machine at rest
- B : non loaded machine manually rotated
- C : loaded machine -50Hz 1 A supply- at rest
- D : loaded machine synchronized with a 50Hz 1 A supply.

A: The leakage field is stronger on position 1 and 2. It sounds normal that we almost do not feel any field leakage on 3, the flux circuit is better closed over there.

B: As much as we rotate manually the machine, the location 3 does not modify its previous results. Although, either location 1 or 2 gives sinus waveforms whose frequency is of course in respect with the speed and the number of magnets.

➔ In our seek of PM flux detection, Location 3 already disqualifies.

C: Location 3 is subject to a well visible sinus field.
Locations 2 and 3 seem to get a small sinus around their previous values.
It is then mainly the stator flux that is sensed around the old constant PM flux value.
Location 3 is much more sensitive because very close to the loaded coil.
It is a direct image of the current, then, the response time of the sensing device is measured thanks to the phase shift between the real current and the sensor output. Td=0.2ms
The field sensed at location 1 and 2 is no longer directly the one emitted by the coil directly but it is the leakage field of this stator sinus field flowing through the magnetic core.

D: Finally, before and when getting the synchronism, location 3 obviously give pretty much the same last results. However, position 1 and 2 provides a signal like an addition of different frequencies sinus before until some 50 Hz sinus with larger magnitude shows up once synchronized.

This stator flux sensed is undesirable because it can fake the PM flux detection.
The point is to sense the maximum PM flux and the minimum Stator flux.
The highest PM flux contribution appears over position 1 and 2 when the sensor is close to the air gap- yellow belt on the figure.
To determine the final best position, the influence of the stator field according to the location over this yellow belt between 2 poles is studied.

For every position a short interval of the sensor output is plotted, meanwhile the machine is electrically loaded at rest.
Finally, the maximum and minimum value assumingly representing the peak-to-peak stator field sensed are caught and plotted below for every position.

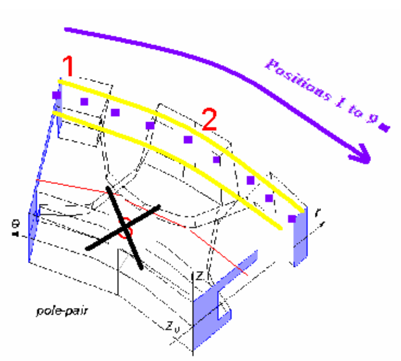

Figure 32 : Stator Flux Measurement versus 9 positions

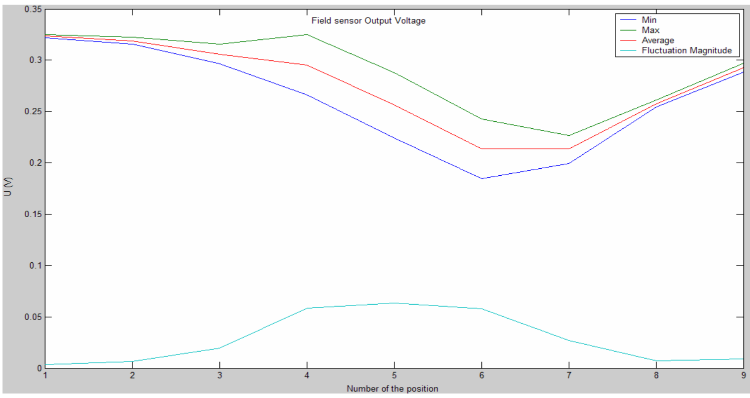

Figure 33: Stator Flux Influence Versus Position

The figure is quite clear: the positions between 2 poles disqualify.
It also says that the closer to the middle of a pole, the lesser stator flux is sensed.

Moreover, by handling the real machine, when the sensor is at the middle, the last assumption is confirmed, the absolute maximums of the field signal seems to correspond to the unstable positions, which are the ideal polarities change positions of the machine.

The exact middle of a pole very close to the air gap is the best position.

4.4 Different methods for the actual control

Below is the scheme gathering the different possible methods for the actual control

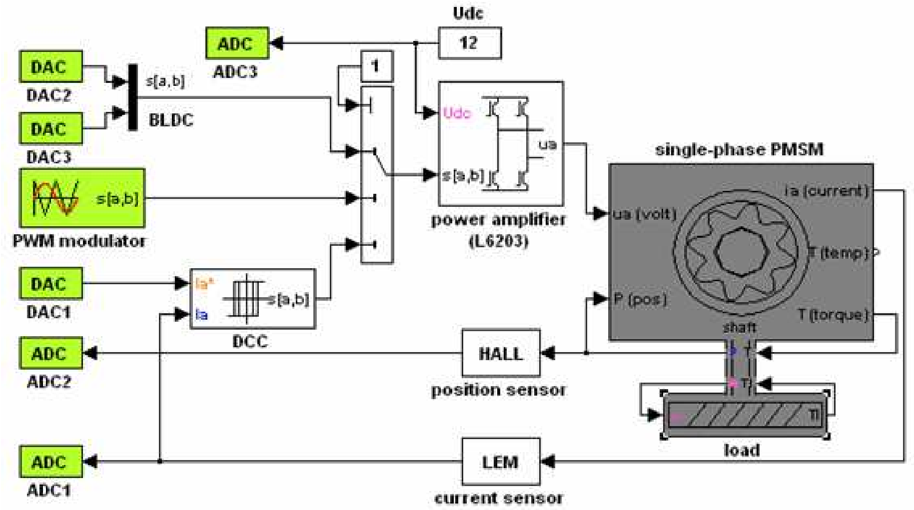

Figure 34 : Control Scheme with microcontroller inputs and outputs

The synchronization control strategy gives the basics of the control but the total implementation can be implemented in several ways:

a. Brushless dc (BLDC) drive where the control via dspace decides a switch state of the power amplifier.

b. PWM modulator in dSpace specifies the switch-state of the power amplifier according to the input reference voltage formed in the program every sampling time. The current can be controlled -Sampled Current Controller (SCC)- or not.

c. Direct current control (DCC) that only need a single input from dSpace as a reference current waveform.

The necessary input from the drive circuitry is

d. rotor position sensed by a single a few hall elements

e. armature current of a single-phase PMSM to control its level for safety reasons, or process SCC.

The output from dspace are:

f. the switches triggers signals for BLDC or PWM control
g. the current reference if DCC control

Every possibility is simulated on Matlab.

5 Simulations of the actual machine

Below is the final matlab model used for the simulations of the actual machine.
The leftmost side gets the different elements of the control: sensor, signal treatment, PWM until the 4 quadrant converter. The rightmost part deals with the electromagnetic and mechanic behaviors of the machine.
To stick the most to the experiments to be implemented, the parameters are selected or estimated as close to reality as possible.
Like in most of the experiments, the maximum DC voltage is Udc=30V
R=11Ω and L=24mH are used as electrical parameters
The inertia is calculated like any rotating ring J= 5.3 g.m^2.
The Damping D is estimated considering the average value of the mechanical equation (5), when the machine stops to be supplied at a steady-state speed.
That is, with T=15s, D=J/T= 0.353 N.mm.s
As the different methods give basically the same results, the results shown below are those of the PWM control implemented in practice: It is used with Ts=1ms as sampling period rather than 0.1ms which is too demanding in term of calculation for the computer.

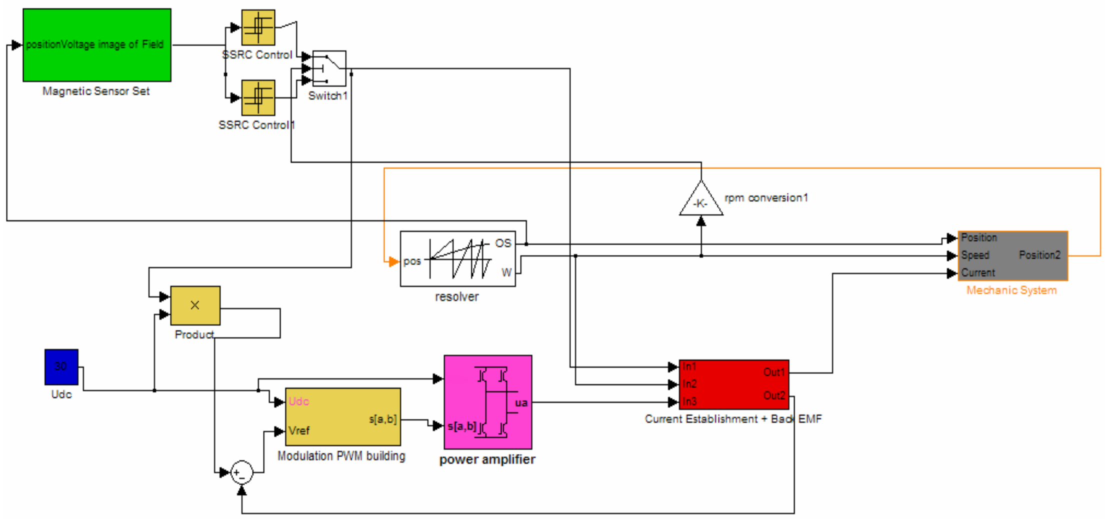

Figure 35 : Matlab model in the case of PWM control

The most interesting parts to focus on are:

-The starting conditions,
-The evolutions of the torque, current, and speed all along the run
-The verification of the synchronism keeping when applying load torque

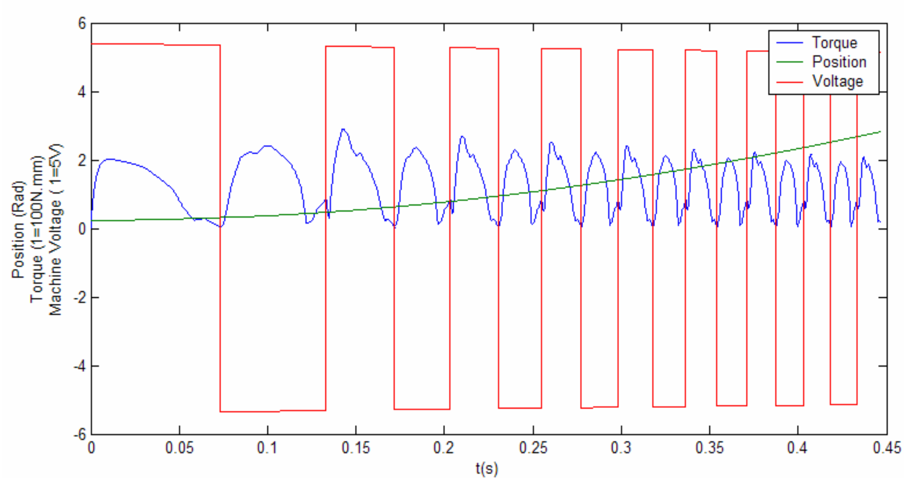

Figure 36 : Simulated Starting Conditions for Udc=30V

Like expected, a first positive voltage pulse is ordered in concordance with the field detection, triggers the first move thanks to positive torque, until the field reaches the next maximum, which triggers the negative voltage pulse, and the continuation of positive torque and of the acceleration and so on. The machine gets started.

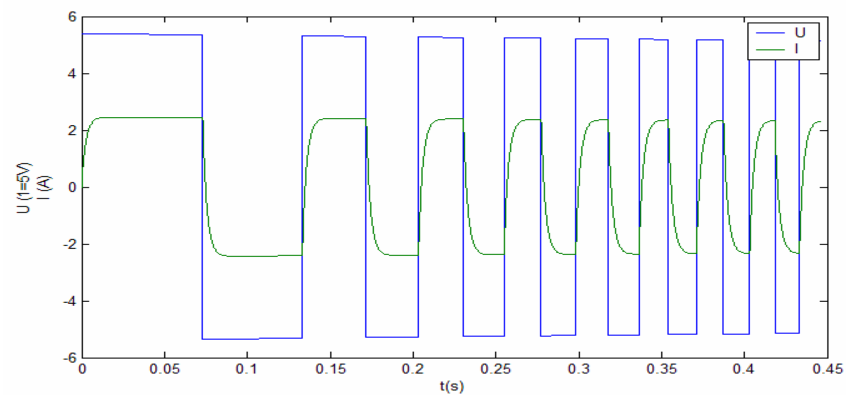

Figure 37 : Simulated Voltage and Current during starting

On -*Figure 37*-, the current establishment is well noticeable. Furthermore, this figure tells that after half a second, the current can no longer be considered as a square wave, but it is getting more and more like a triangle whose peaks are situated at the pulse changes.

These peaks are naturally consequently reduced as much as the speed increases because the pulse width is consequently decreasing and because the back emf is increasing too.

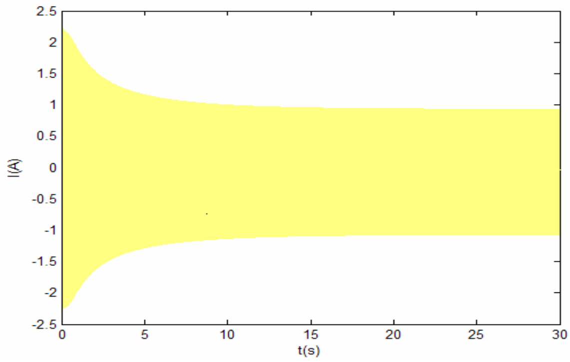

Figure 38 Simulated current along an entire run

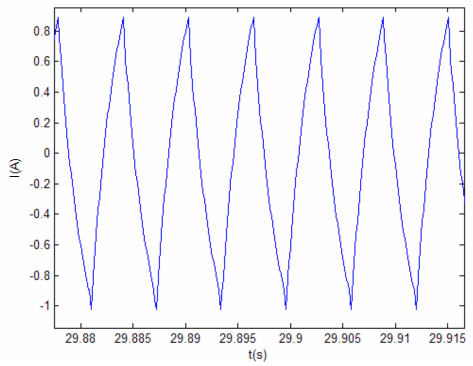

Figure 39 Simulated current when "steady state" is reached

The current peaks at the beginning are quite high (superior to 2 times the nominal rated value). It can be either considered acceptable for a few seconds or some special starting conditions can be set, giving like a percentage of the actual reference voltage.

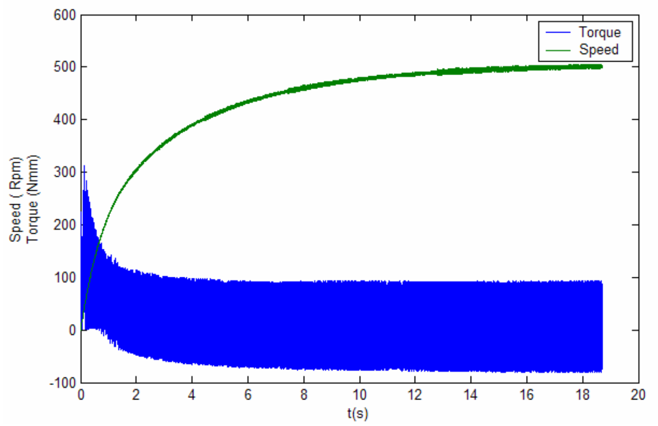

Figure 40 Speed and Torque along the run

The maximum speed in this case is 500 RPM.
The torque is quite high at the beginning with full high level square current pulses and drops like the level of the current until the electro-mechanical equilibrium is found.

Below -*Figure 45*- is what happens in a case of load torque changes or perturbations:

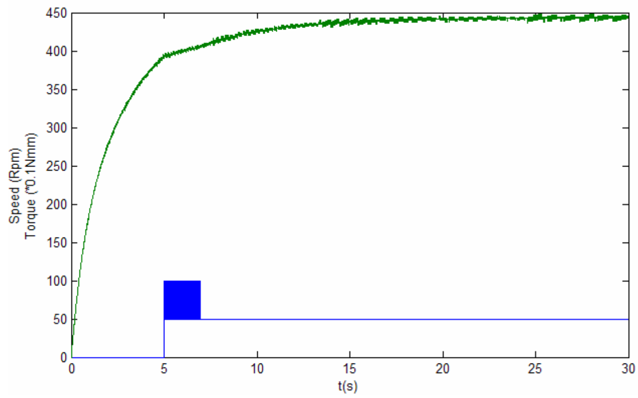

Figure 41 Keeping of Synchronism with load torque

The control is pretty robust and seems not affected by torque perturbations.

To conclude with the simulations:
-the machine gets started,
-in the good sense,
-it keeps synchronized.
Regarding the final speed, these described phenomenons of decrease limit the speed as they are interdependent. In this prospective, a further study is done to identify and overcome these limitations.

6 Limitations of the speed

When designing a machine, the range of maximum speed to reach is estimated.
But the speed is limited by a quite big numbers of parameters.
The first is obviously physical. Indeed, even if the ideal conditions (set in the previous model) were real, at the nominal current pulses -1/1A, the machine has a maximum average torque and energy, which gives an absolute maximum speed according to the dynamic equation (5).
The other ones are due to detection problems and electro-magnetic limitations.

6.1.1 Area Detection Limitation

First the area detection on which our method is based cannot be perfect
In order of importance the signal treatment time (certainly very small though), the time response of the hall sensor, (Td=0.2ms), the "cannot be perfect" placement of the field device (slight move of the sensor = big change in sensed field), can triggers a quite big shift between the actual and the expected pulses, and then a quite big loss of torque and reachable speed. -*Figure 36*- The wider the shift is, the higher the losses are, and the slower the machine runs.

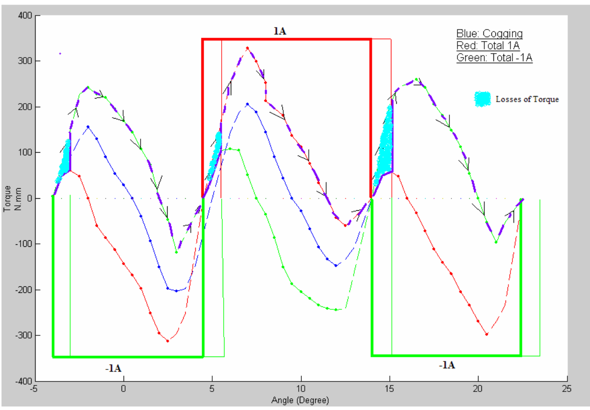

Figure 152: Torque Losses with delayed pulses

6.1.2 Current Establishment Limitation

When a current pulse is ordered, the 4 quadrant switches in such a way that there is a corresponding voltage over the machine. Then, according to its resistance and its inductive phenomenon varying with the speed, the current gets its expected value after a certain time.
In this prospective, the electromagnetic equations of the machine can be first well approximated by a simple R-L Circuit. Thus it can be assumed that the establishment of the current is almost

done within 2 times the electric constant T=2*L/R. -*Figure 36/37-* Numerically, with the real measured parameters L=0,024H and R=11Ω, T=4,4 ms.

(6) $U = R \cdot I + L \cdot \frac{dI}{dt}$

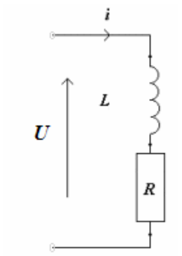

Figure 43 :RL Circuit

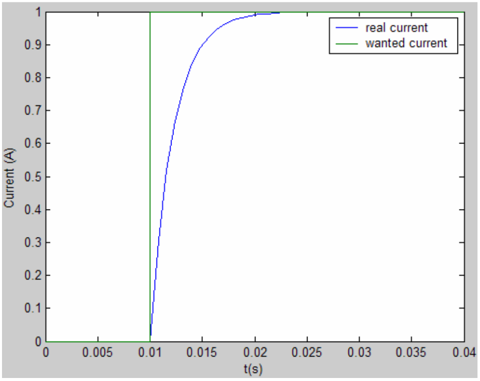

Figure 44 : Current Establishment

This period when the current is lower than wanted triggers a quite big loss of torque.
For instance, at the switching position 0.15 rad on -*Figure 39*-, instead of switching instantaneously from the blue area to the red one, this makes the torque keeping a while in the blue area -negative or low torque in 0.15/0.30 rad-, crossing the yellow one -low/middle level torque - before reaching the red one.
Furthermore, if the electrical frequency is higher than f=1/(2T)=113.5Hz which corresponds to a speed Ω=340 rpm, then the current never reaches its expected value.
Therefore the final average torque and consequent final speed is much lower than it could be.

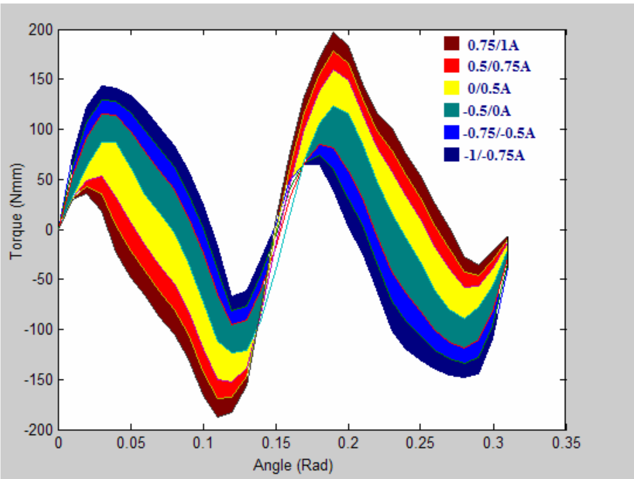

Figure 45 : Torque Versus Current

6.1.3 Back Emf Limitation

One other important issue in the modeling of the machine is the flux management and the back EMF. Indeed, according to Lentz law, the machine produces the opposing back EMF which is proportional to the variation of the total flux (9).

Electromagnetic equations:

(7) $U = E + R \cdot I + L \cdot \frac{dI}{dt}$

(8) $\Psi = \Psi pm(\theta) + \Psi elm(J, \theta)$

(9) $E = N \cdot \frac{d\Psi}{dt}$

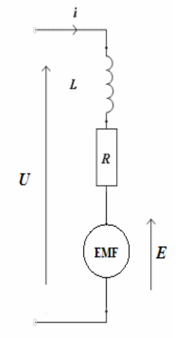

Figure 46: RLE Circuit

Like it was highlighted when running the machine, the PM flux and the stator flux are synchronized to give a sinusoidal total flux whose frequency is proportional to the speed. Consequently, the back EMF peak is proportional to the speed too.

According to some measurements previously done - *See Annex 3* - the coefficient back EMF/speed is available and its evolution is plotted below as well as the resulting total voltage Udc needed with 1A flowing into the machine -*Figure 49*-.

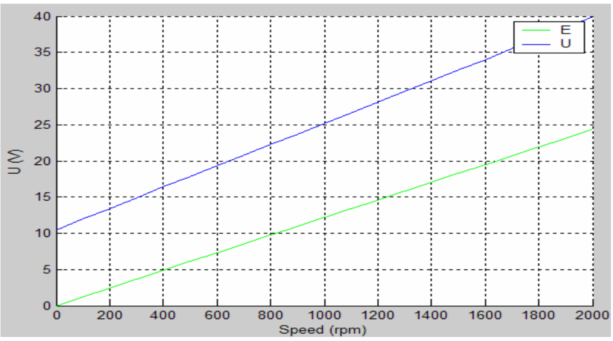

Figure 47 : Back EMF and Udc needed for 1A peak

Thus, as much as the speed increases, the back EMF also increases, thereby reducing consequently the available voltage for the current establishment, the average torque, and so the maximum final speed.

The expected value is the appropriate term because the described current establishment time quickly becomes longer than half an electric period. To illustrate this, an example of the evolution of the current at 500rpm (electrical frequency 167 Hz) with appropriate DC voltage is supplied to the system is plotted below.

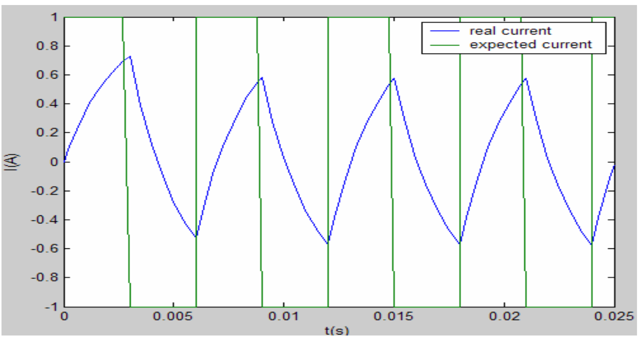

Figure 48 : Example of the evolution of the current at 500

Not only the current takes some time to reach its maximum value but its maximum value is 0.55A instead of 1A expected.
The current establishment seems to be by far the biggest limitation.
Furthermore, the shape of the current plays a big role too.
Indeed, let us assume that the triangle shape of the current has the same torque impact as a square with steps to 0. *Figure 49-*.

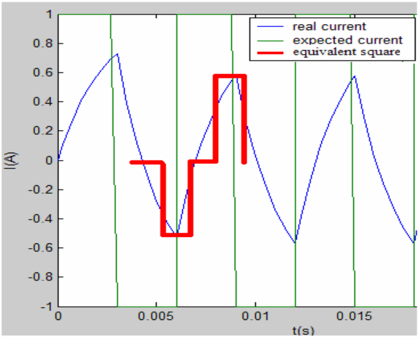

Figure 49 : Equivalent Current Square

We figure thus that the times with the highest current correspond to the ideal changes of polarities, meanwhile the part with the highest torque are only close to cogging in this configuration.
Having a look at -*Figures 42 and 45*- is enough to assess of significant losses of torque.

6.1.4 Pushing up the limitations

Increasing again the DC voltage so that the current peak can reach a higher value is a first solution but the voltage magnitude is limited by short circuit and the coil insulation.

It does have a positive impact in the sense it allows more voltage available in the current building, but it has no impact at all against the area detection limitation and the current establishment limitation.

Thus, another idea is to advance the signal detection, and so the current too: Phase shift advancer.

First, it compensates the unwanted delay of the area detection evoked below.

Then, the phase shift advancement allows concentrating the best part of the current on the best part of the torque characteristics. *Figures 50 and 51*.

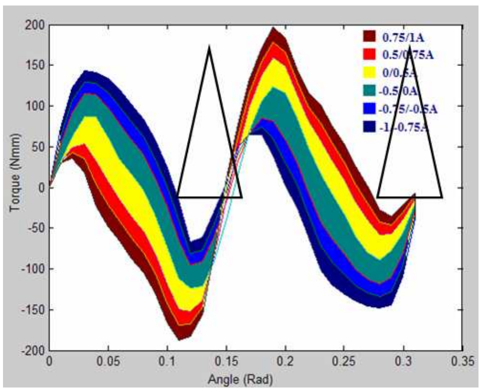

Figure 50 : Torque Selection with current Without phase shift

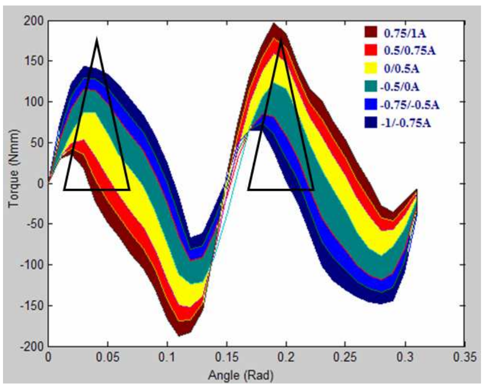

Figure 161 :Torque Selection with current With phase compensation

This way, we take all the best that the whole system can give.
It sounds quite complicated to advance a signal compared to late it, but it is feasible. Chapter 7.2 explains the method used for that.

7 Experimental work

7.1 The electronics and power electronics

Regarding the choice of power electronics, the criteria taken into account are common:
- Pretty high frequency
- Suitable power rating, which is not too high here (below 50W)
- Low cost

The device L6203 is chosen because it fits with all the requirements and is at disposal.

On Annex, is presented the electric scheme of the DCC control as well as the current measurement part.

Another electronic part is also done to convert the 15 -15V of the dspace PWM into 0-5V for the switch trigger signals

7.2 Writing of the C-code

The whole programmed C-code is written in Annex.

Once the variables are declared, the starting part sets the variables and allows the main part of the program to be repeated every sampling time Ts=5e-5s.
The most important parts are going to be detailed:

- The binary pulses building
- The speed estimator
- The phase shift advancer

<u>The binary pulses building</u>

Rather than deriving, which always leads to secondary problems, another idea to detect the maximum of the field is imagined:
The maximum is the point where the older sampled value is lower and the next sampled value is higher.
Then a very good approximation is to order the change of polarities when
Old Old Value< Old Value
Old Value>New value
It is exactly the contrary inequalities for the minimum peak.
Thus the ideal pulses are already shifted from one sampling period but it is not so big shift and for high speed it can be arranged back with the shift advancer.

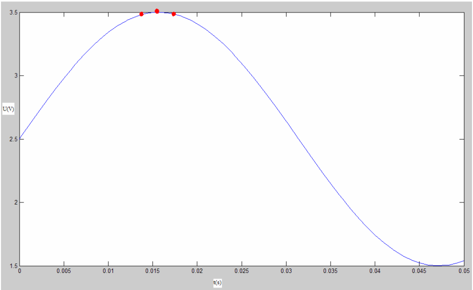

Figure 52 : Pulse Detection Method Illustration

Yet, the signal is very noisy and without any changes, it leads to perturbations and a lot of unexpected change of polarities.
A low filter is implemented, the choice of frequency calls according to cut and try. A compromise has to be chosen between the importance of the phase shift inherent to the low filter and the remaining noise of the signal.

Still with this cut and try thinking, another condition is added for the change of pulses, the field signal must be superior (respectively inferior for the minimum peak) to a certain level.
Once well determined, this condition has 2 advantages:
The pulse changes are only ordered when the machine is rotating or going through the other position area and not oscillating in the same zone.
Well associated to the low filter, it seems to remove totally the unexpected polarities changes.

From, this binary signal, and according to the conditions and the speed, some different current references can be set.
For instance, it is acceptable to have a higher current during the starting period, and then go back to nominal rated value.

The current reference leads to a voltage reference, and the duty cycle of the PWM signals are calculated as proportions of the DC link voltage

<u>The speed estimator</u>

To be able to have an image of the speed evolution and to know the reached speed, a speed estimator is created:
The way pulses building has been processed, a period of the pulsed signal corresponds to 18 mechanical degrees. Then, the speed can be well estimated finding out the time spent by the motor to rotate around one or several areas. To have an instantaneous value, both counters for the time and the number of periods or areas are regularly reset to 0.
Another version is done with the current every time the current go through zero (old value negative and new positive)
Both methods are working pretty well, but they are dependent on the good running of the pulse building. Regular missing in the area detection directly leads to fake speed estimation.
The speed estimation can be used if the controller takes the back emf into account and is used in the phase shift advancer

The phase shift advancer

The phase shift advancer is made as a second step in the running, first because it could not work at the very beginning and because it is of a bigger interest to compensate the different late shifts when the speed is already pretty high.

Here is how it works.
A real-time calculation of the number N of sampling time per pulse (or per half a period) is done based on the speed estimation, which in rpm is 3 times the electrical frequency. Thereby, it leads to:

(10) $N = \frac{3}{2 \cdot \Omega \cdot Ts}$

Thus, one way to implement the phase shift is to order the pulse change before this number N.
To do so, a counter starts every time the real pulse alternate.
Then, the pulse change is ordered when the counter is below a certain percentage of the calculated number N.
As N is a real and not an integer, the change occurs when the counter is framed between the percentage times N and the percentage times N minus 1.

This percentage coefficient is 0.9 – alpha.
The 0.9 part is partly there to ensure that the eventual speed calculations errors will not make a pulse missing.
The alpha is setting the phase shift, which we can modify manually during the run. Indeed, in term of angle, this way, the phase shift is directly 0.1+alpha radians.

This method shows very good results in the phase shift.
However, the compromises of the 0.9 coefficient and the frame inequalities have to be well taken care of in order not to miss any pulses at any speed.

7.3 Results

The all strategy using dspace interfaces and the PWM method is now implemented for real on the machine which gets a ventilator part, which corresponds to a load torque.

Starting and Keeping of synchronism

The implementation of the PWM method – with Vref control – makes the machine start rotating whatever the initial position.
Below are plotted the starting conditions with Udc=15 V.

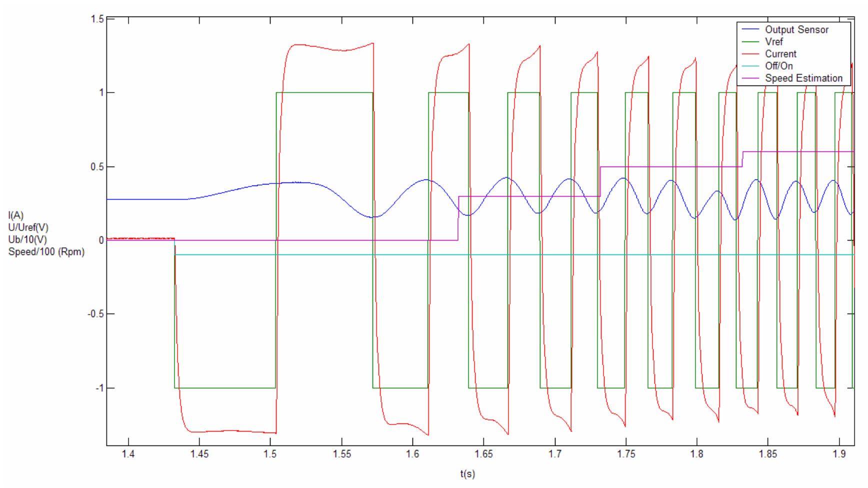

Figure 53 : Starting conditions in practice Udc=15V

The pulse buildings are like we expected.
However, we can notice that the field is not a perfect sinus but the maximum and minimum values vary according to the positions, which explain the difficulties in the writing of the pulses detections C-code.
Exactly like we saw in the simulations, the current turns very quickly from a square signal to a triangle whose peak is getting smaller and smaller,which confirms the need of a phase shift advancer.
The weird shapes of the current close to the pulse changes are due to inherent filtering in the current acquisition.

The machine never loses synchronism if we apply some opposing torque or perturbations, as long as the torque applied is in the range of torque that the machine can produce.
We can figure that this “simulated” torque variations trigger increase of current. It is normal since the speed decreases – more current establishment- and bigger load torque is always more demanding.

However the sense of rotation depends on the initial position, which is certainly due to the fact the field is not a perfect like theoretically and the initial value supposed to help the determination of the sense for the starting varies too much according to the positions.
A way to definitely remove this unconvenience is to use 2 sensors, this way, the sense can be determined from the beginning observing the shift between both sensing signals and the right pulses can be consequently sent.

<u>Phase compensation effect</u>

The first shot with Udc=30V gives 300RPM - *Figure 54* - meanwhile the simulations indicated about 500RPM, and this final speed is reached a bit faster than in the simulations.
It is certainly because of the too rough estimation of the mechanic parameters, but also because the delay in the pulse building was not taken into account in the model. Finally a third explanation is that we didn’t consider the load torque created by the ventilator in the simulations.

A second try implementing the phase shift advancer in a second part of the run makes the speed immediately goes up to 500 RPM - *Figure 54* -, and emphasizes the importance of the phase compensation for getting better speed.

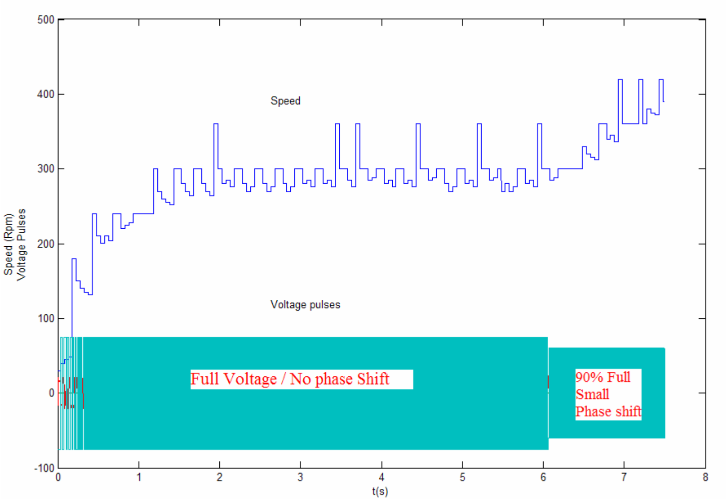

Figure 54 : Speed Evolution along a normal run and effect of a small phase compensation

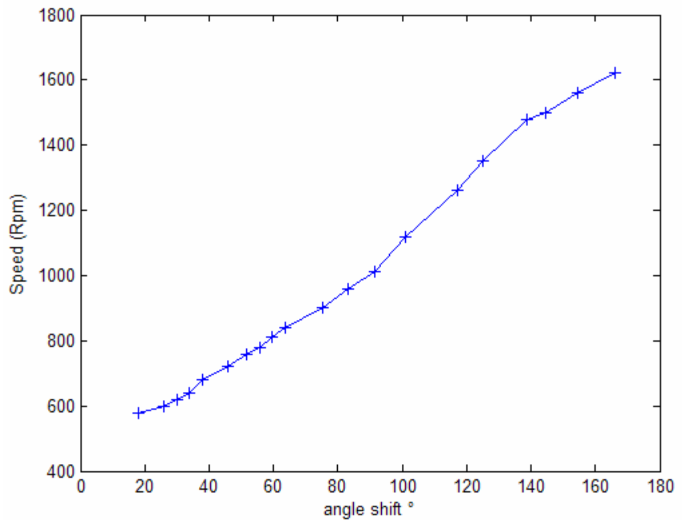

Figure 55 : Speed versus Phase compensation

As much as the phase compensation is increased, the speed considerably increases too up to about 1600 rpm.- *Figure 55* -.

However, right after 180 degrees angle shift, the machines loses synchronism. Indeed the signal is no longer in phase compensation that the switching times are all wrong.

During these phase and speed increases, the current peaks are logically decreasing, and their widths get smaller too -back emf and current establishment effects-.

However when reaching the maximal speed, the current describes roughly a sinus whose peak seems to be slightly higher again.

It is likely that this phase compensation makes the fields almost perfectly synchronized and that the current gets the same waveform as the back emf which is almost a sinus.

The irregularities observed at middle high speed with middle range phase compensation in the current shape may be partly due to the fact that some positions are ridden faster than others, because of the torque irregularities.

The current at those speeds are very low – about 0.1/0.2A-, much above the 1A expected still because of the high back emf and the current establishment effect.

Increase of the DC link voltage:

From a full phase compensation state, the dc voltage is increased from 20 to 50V, the results are displayed on *Figure 56:*

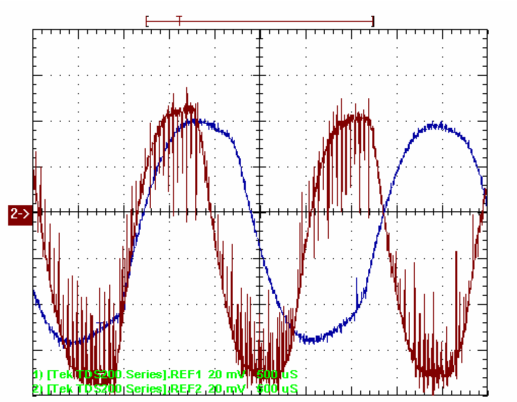

Conditions:
Udc 20V(blue) & 45V (red)
RMS 38.69mV & 47.98mV
Pk-Pk 103.2mV & 140mV
RiseT 0.496ms & 340ms

Figure 56: Currents measured with oscilloscope

Udc [V]	n [rpm]	Idc [A]	Freq [Hz]	Ia CycRMS [mV]	Trise [ms]
20.0	1200	0.28	400	37.7	0.58
25.0	1320	0.29	441	41.6	0.44
30.0	1420	0.30	475	42.5	0.42
35.0	1500	0.31	499	43.8	0.39
40.0	1560	0.31	511	44.5	0.39
45.0	1600	0.32	529	46.0	0.36
50.0	1680	0.35	550	48.8	0.34

Increasing the DC voltage generally tends to increase slightly the current peak and decrease its time rise, and so contributes to an increase of speed and frequency.
These parallel phenomenons are not regular and proportional though.

Both signals with 20V and 45V looks roughly like a sinus. The first on which the phase has been first set seems slightly more like a sinus though.
It is likely that the phase shift that gives the absolute maximum speed for a certain DC voltage, which corresponds to "perfect synchronization", is not exactly the same for a higher DC voltage.

Power Prospective

The total power supplied to the system can be seen on the DC supply.
A try without the ventilator part is implemented.
As the "output torque" is reduced, the speed is higher.
A decrease of around 0.03A in the current can also be noticed which gives the mechanic energy taken by the ventilator, or useful power: 0.03*30#1W.

The total power in comparison is about 7.5W Udc=30V I=0.25A.
Some of this power is used for mechanic equilibrium: production of the torque compensating the damping torque.
Most of the differences can be explained in term of losses, the supply of the circuit taking 0.04A, switching losses and voltage drop of the power converter, resistive losses 0.7W and magnetic losses of the machine.

8 Conclusion

In this paper, a method to control a single-phase claw-pole machine has been designed and has given very good results.

Most of the objectives have been met:
-Starting up the machine whatever the initial position
-Keeping synchronism whatever the perturbations
-Reaching High Speed
The non-satisfying objective of the direction choice is due to a shift between theory and practice, and a way to overcome it can be implemented.

From this work, the very good way of working of Hall sensor as position sensor on a quite big range of frequencies is highlighted.

This passionate thesis work with which I learned a lot on a personal prospective is not an end to the project led by IEA. The future work will consist of reaching higher speed limitations through further understanding of what is really going on, and designing a more efficient fan machine.

References -apart from the general information from the IEA department-

[1] Design of Powder Core Motors, Avo Reinap

[2] In-depth Learning of Cogging/Detenting Torque through Experiments and Simulations
Tatsuya Kikuchi, Member, IEEE, and Takashi Kenjo, Member, IEEE

[3] Cogging Torque reduction in a permanent magnet wind turbine generator
E. Muljadi J. Green

[4] Prediction and measurement of the detent torque of a single phase machine
E Santander, A Ben Ahmed, M Gabsi

ANNEX

1)Additional observations during measurement for Magnet Ring 1

- I≠0 We can figure a real symmetry and periodicity, the symmetry is central around 4.5 degrees and the scheme is 18 degrees periodic, that is the scheme is repeated every 2 stable positions, or in other words every pole.
- I≠0 Applying +-1A from the other stable positions of torque make –most of the time- jump the position to the next stable position, the sense of the jump depending on the sign of the current applied.
  For instance, from 9°, 1A leads to 13.5° while –1 A leads to 4.5°.
  And from 0°, 1A leads also to –4.5° while –1A leads to 4.5°.
  From 0°, with 1A, the jump can be described this way, it first try to reach or join -6.5° which is an unstable position, and then it oscillates around -4.5°.

When handling the machine, trying to feed it with "manual" current pulses, like connecting/disconnecting the machine with 1A supply, we feel the importance of the passive stable positions.
Not only, if it is started from them, it doesn't move an inch, but when starting elsewhere, we feel that there is a limit time to change the polarities. In other words, when it is too much in the oscillation around the dead position, it is too late to move the machine again.

2)Additional observations during measurement for Magnet Ring 2

Once 1A or –1 A applied, the resting positions don't follow the same scheme. Instead of unfolding every 9 degrees, they are 2 resting positions quite close to each other from 5 to 5.5 degrees while the following resting position is situated from 13 to 13.5 degrees further. More clearly, "-1 A setting" has its resting positions as follows:
-10.5 / 2 / 7.5 / 20 / 25.5 and so on…

From the plotted measurements, we figure several observations:

- The cogging torque peak level is much higher than for the magnet ring 1 like expected. Numerically it is around 1.5 times higher
- We can figure a real symmetry and periodicity for both cogging and total torque, the symmetry is central around every unstable zero torque position and the scheme is 18 degrees periodic, that is the scheme is repeated every 2 stable positions, or in other words every pole.
- It appears also that the zero torque unstable positions of the cogging torque are actually common points and unstable positions whatever the characteristics drawn. Some quick tries with 2A show us they might be common unstable positions whatever the current applied, at least in a reasonable current range.
- The torque peak when +1A applied is higher than it is when –1A.

From a stable position, we can follow the shift or displacement of the machine when progressively applying some current from 0 to 2A. Thus, it provides us the different resting positions according to the current applied. Below is the resting position according to the current around 0.5 degrees.

I(A)	0	0.15	0.3	0.5	0.85	1	1.5	2
θ	0.5	0	-0.5	-1	-1.5	-2	-2.5	-3

Running the machine with a 50Hz sinus by trying to get handy the synchronism, we figure that the vibrations are quite intense and the noise loud.
However, increasing the magnitude of the current reduces it significantly.
At slightly higher frequencies the noise is reduced too.
We already figure that vibration and noise are highly dependant on the current and so on the match cogging/drive torque as well as on its frequency.
Indeed some mechanic vibration harmonics can be excited.

3) Calculation of the back EMF/speed coefficient

Some measurements of the induced voltage were previously done at different speeds on digital oscilloscope and then integrated over a period the following led to the following curve. Thus, a good approximation for the coefficient relating the back emf to the frequency is the fundamental value of this measured signal.

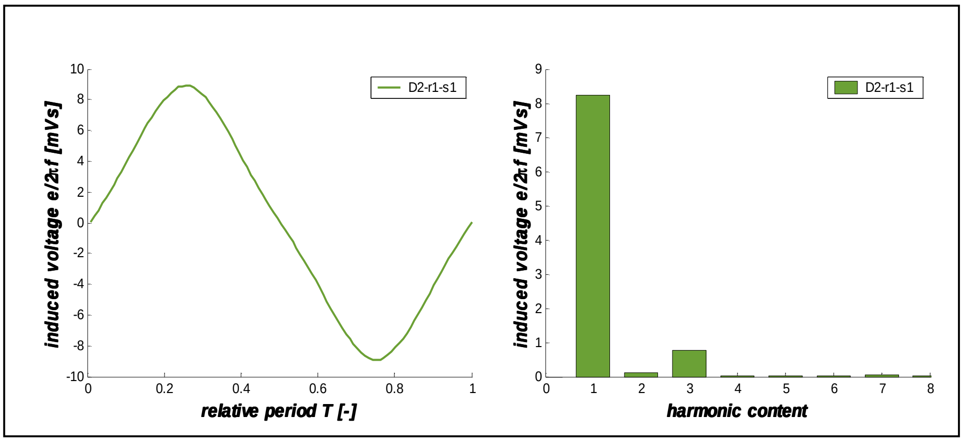

4) Electronic Circuitry for every control solutions

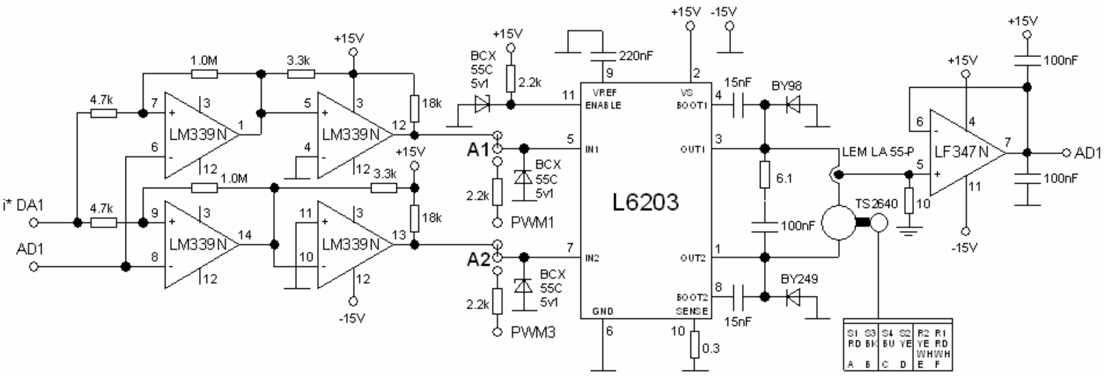

On the left, the DCC circuit based on hysteresis amplifier. Comparison of i*DA1 from dspace and AD1 the actual current.

In the middle the 4 quadrant devices and the protective components.
PWM1 and PWM3 come directly from dspace for brushless and PWM control.

On the right the machine, the LEM with its current measurement system

5) Final C-code (Only most of the calculations useful for the run are shown)

```
(…)
 /*--------------------------------Read from ADC------------------------*/
 ds1104_adc_start(DS1104_ADC2|DS1104_ADC3|DS1104_ADC4|DS1104_ADC5);

 ds1104_adc_read_mux(scantable, 4, u);
 //Udc = u[3];  //Multiplexed chanals

 i = ds1104_adc_read_conv(3);  //AD6

 H = ds1104_adc_read_conv(2);  //AD5

 /*--------------------------------Filtering--------------------------*/
 //LP-filter1 4Hz
 H1 = ((H-H1_old)*w1*Ts)+H1_old;

H2=H1;
H3=H2_old-H2;
H4=H3_old;
H5=H4_old;
```

```
  /*--------------------------------Calculations-------------------------*/
//Starting phase before N=500
//Second phase of pulse building S2>500

if(H3>0 && H4<0 && H1>0.32 )
      {X=-st;

      }
 else if(H3<0 && H4>0 && H1<0.21 )
     {X=st;
    }
if(S2>500)
 {if(H3>0 && H4<0 )
      {X=-st;
      }
 else if(H3<0 && H4>0 )
     {X=st;
      }
 }

// Phase compensation started after N=500

if (N==500 && ((X==-1 && X_old==1)||(X==1 && X_old==-1)))
       {N1=1;
       };
 if (N==500 && N1>0 )
       {N1=N1+1;
       };

if (N<500)
   {if (X==-1 && X_old==1)
        {N=N+1;N2=N2+1;
i_ref=1.5*Ir*X;
}
else
   {if (X==-1 && X_old==1)
        {N1=1;N2=N2+1;
        };
if (X==1 && X_old==-1)
        {N1=1;
        };

if(N1>=((0.9-alpha)*3/(2*S2*Ts)) && N1<=((0.9-alpha)*3/(2*S2*Ts))+1)
 {i_ref=-1.25*X;
 }

if (i>0 && i_old<0 )
```

```
      {N3=N3+1;
      };
    }
//phase shift calculation
Psc=(0.1+alpha);
Psd=(0.1+alpha)*180;

X1=(0.25*X+0.5)-0.25;
X2=-X1_old+0.625*1-0.15;
//PWM solution 1

uref=R*i_ref;

if (uref>Udc)
  {uref=Udc;
  }
if (uref<(-Udc))
   {uref=(-Udc);
   }

//Speed Estimation

C2=C2+1;
if(C2==1000 || C2==2000 || C2==3000 || C2==4000 || C2==5000)
{S2=(N2/20)/(C2*Ts)*60;
 S3=(N3/20)/(C2*Ts)*60;
}
if (S2<10)
{S2=0;}
if (S3<10)
{S3=0;}

if (C2>5000)
{C2=1;
 N2=1;
 N3=1;
}

//Calculate the reference values for the three phases

  /*---------------------------------PWM duty cycle----------------------*/
  duty1 = ((0.5*uref/Udc)+0.5);

  duty2 = 0 ;
  duty3 = ((-0.5*uref/Udc)+0.5);
  if (duty1>0.5)
  {duty1=(duty1+1)/2;
```

```
  duty3=(duty3)/2;
  }
 if (duty1<0.5)
 {duty1=(duty1)/2;
  duty3=(duty3+1)/2;
  }
 // Current safety
 if(i>imax)
 {on=0;}
 /*----------------------------------Write to the DAC--------------------*/
 ds1104_dac_write(1,X1);
 ds1104_dac_write(2,X2);


 /*----------------------------------Update variables--------------------*/
 H1_old = H1;
 H2_old = H2;
 H3_old = H3;
 H4_old = H4;
 H5_old = H5;
 H_old = H;
 X_old=X;
 X1_old=X1;
 i_old=i;
 urefI_old=urefI;
 /*----------------------------------Read execution time------------------*/
 exec_time = RTLIB_TIC_READ();
}
```